Macronutrients CHNOPS	Micronutrients essential to most organisms	Micronutrients essential to some plants	Micronutrients essential to some animals
Carbon	Sodium	Boron	Iodine
Nitrogen	Magnesium	Cobalt	Selenium
Phosphorus	Potassium	Silicon	Chromium
Oxygen	Calcium	Vanadium	_
Hydrogen	Chlorine	_	_
Sulfur	Manganese	_	_
_	Iron	_	_
_	Copper	_	_
_	Zinc	_	_

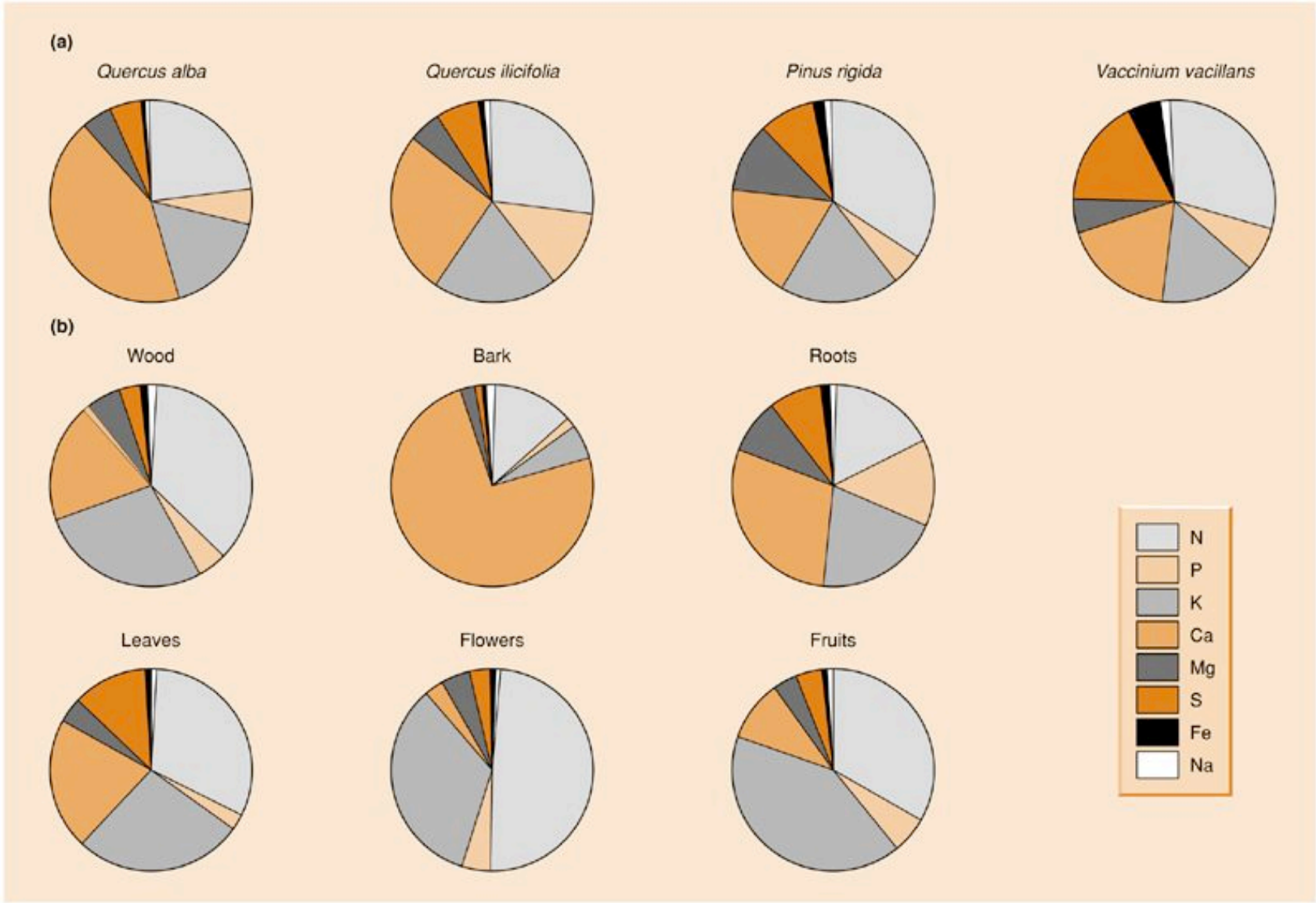

Figure 3.19 (a) The relative concentration of various minerals in whole plants of four species in the Brookhaven Forest, New York. (b) The relative concentration of various minerals in different tissues of the white oak (*Quercus alba*) in the Brookhaven Forest. Note that the differences between species are much less than between the parts of a single species. (After Woodwell *et al.*, 1975).

Element	**Structure/function**
Nitrogen	Nucleic acids (RNA/DNA) Amino acids (protein)
Phosphorus	ATP! Nucleic acids (RNA/DNA) Phospholipids (membranes) Bones
Potassium	Osmotic balance Basis of charge gradients (ATP production, action potentials in animals) Activates enzymes
Calcium	Cell walls Bones & exoskeletons Signal transduction (within cells, between neurons)
Sulfur	Amino acids methionine & cysteine Many enzymes, cofactors, and catalysts Sulfur metabolism
Iron	Ion donor/acceptor (redox reactions, electron transport) O2 transport

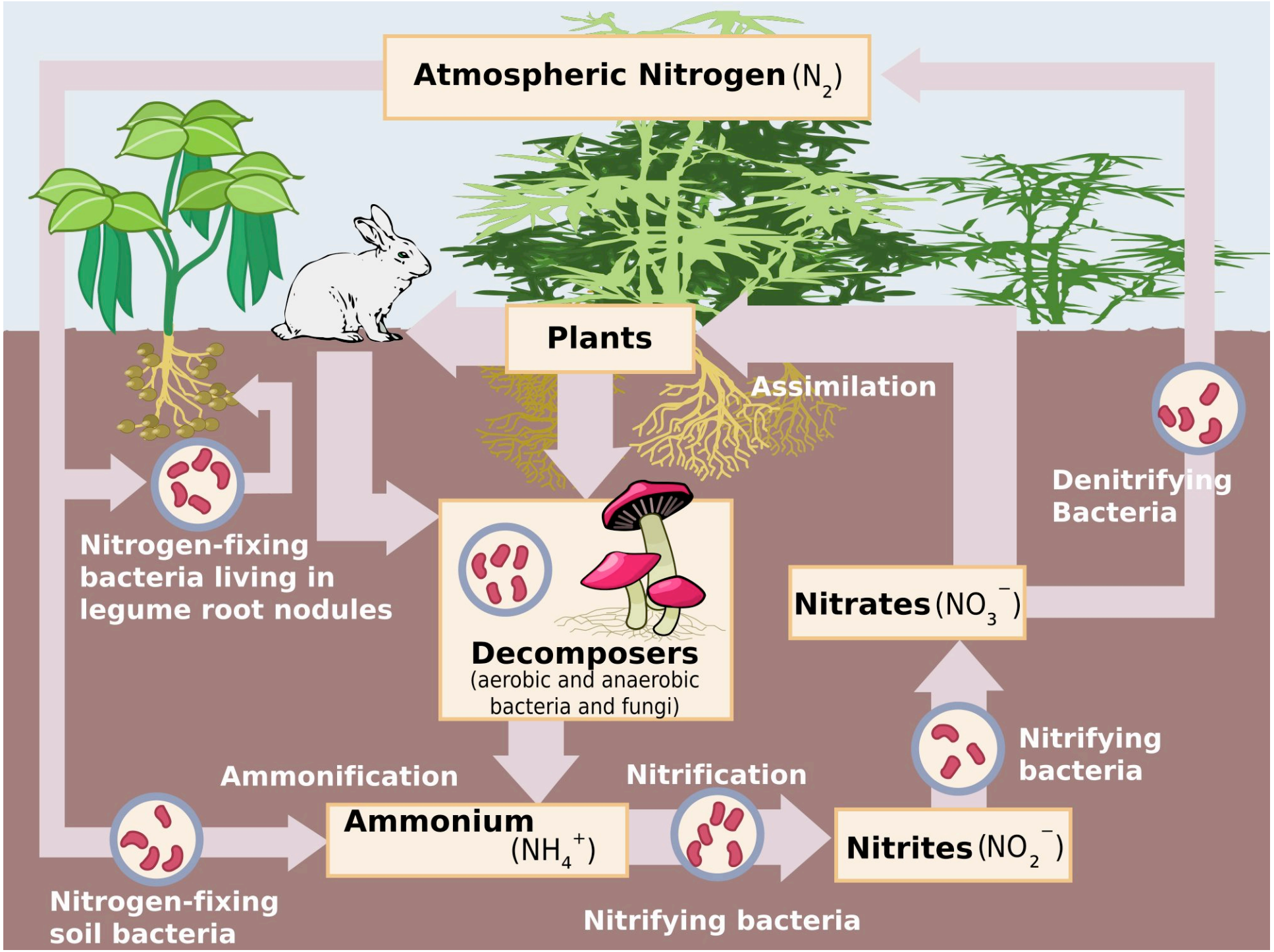
Atmospheric Nitrogen (N_2)
Plants
Assimilation
Denitrifying Bacteria
Nitrogen-fixing bacteria living in legume root nodules
Decomposers
(aerobic and anaerobic bacteria and fungi)
Nitrates (NO_3^-)
Nitrifying bacteria
Ammonification
Nitrification
Ammonium (NH_4^+)
Nitrites (NO_2^-)
Nitrogen-fixing soil bacteria
Nitrifying bacteria

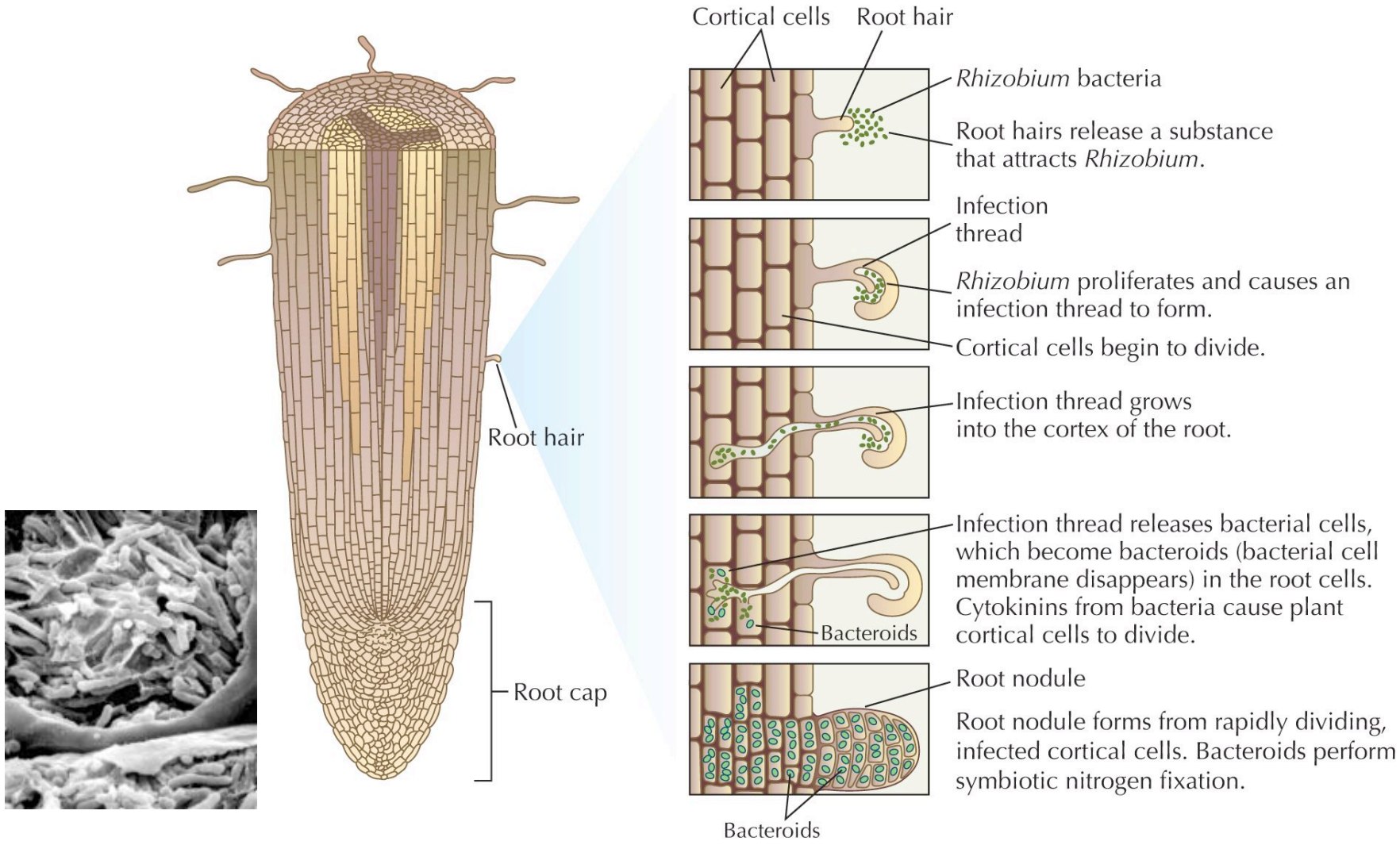

FIGURE 6.26. Symbiosis of *Rhizobium* bacteria with legumes.

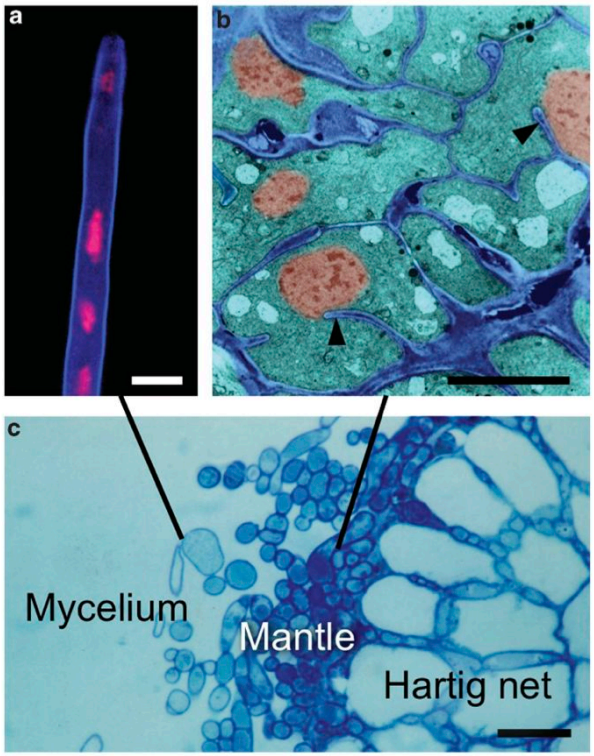

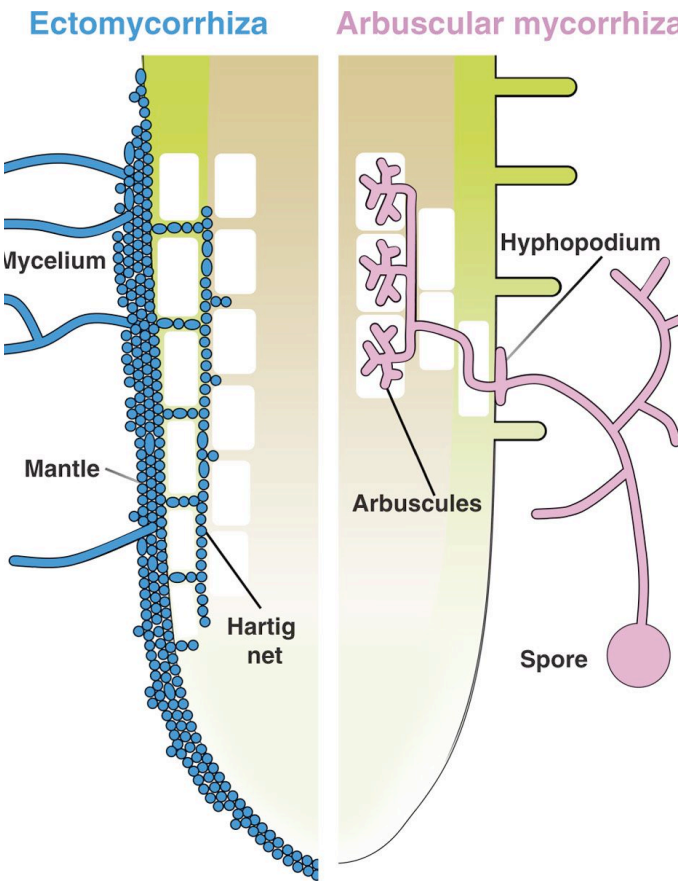

Figure 2 | The transition from the free-living status of an EM fungus to the symbiotic phase. A growing hypha from the mycelium of *T. melanosporum* as observed in fluorescence microscopy is shown in **a** (courtesy: R. Balestrini). Hyphal morphology changes in the mantle, in which the repeated branching, characterized by incomplete transversal walls (arrowheads), originates a pseudoparenchymatous structure, as evident in the electron micrograph shown in **b**. In both images the fungal wall is falsely coloured in blue and nuclei in red. The transverse section of a mycorrhizal root tip stained with Trypan blue is presented in **c**, showing the organization of hyphae in the mycelium, mantle and Hartig net. Bars, 10 µm.

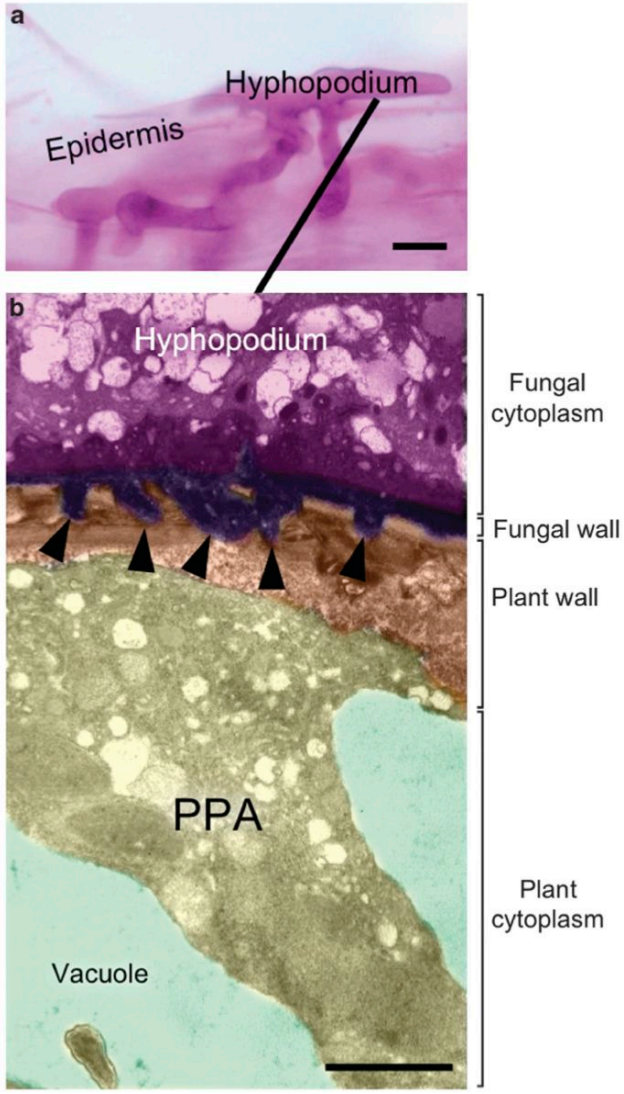

Figure 5 | Hyphopodium adhesion to the root epidermis in arbuscular mycorrhizas. A top view of the carrot root epidermis is shown in **a**, in which a branched hyphopodium of *Gigaspora gigantea* stained with acidic fuchsin contacts the cell surface (bar, 10 µm). The transmission electron micrograph in **b** shows that the hyphopodium strict adhesion to the root is achieved through the formation of several protrusions of the fungal cell wall into the wall of the epidermal cell (arrows). A prepenetration apparatus (PPA), assembled in response to fungal contact, is visible underneath the hyphopodium as a broad column of cytoplasm traversing the vacuole (bar, 2 µm).

REVIEW Published 27 Jul 2010 | DOI: 10.1038/ncomms1046

Mechanisms underlying beneficial plant–fungus interactions in mycorrhizal symbiosis

Paola Bonfante[1] & Andrea Genre[1]

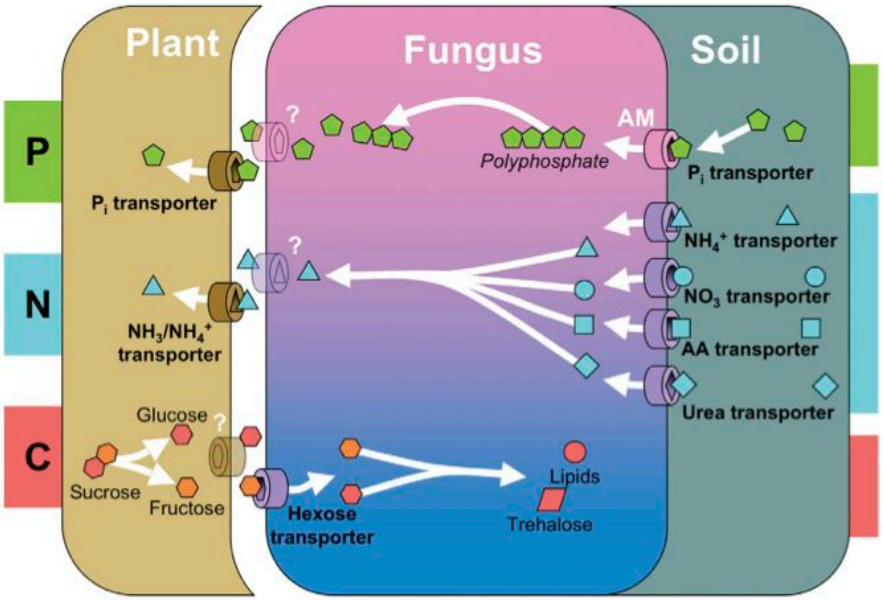

Figure 3 | Scheme summarizing the main nutrient exchange processes in EM and AM symbiosis. Emphasis is placed on the translocation of phosphorus (P), nitrogen (N) and carbon (C) at the soil–fungus and fungus–plant interface. Inorganic P and mineral or organic forms of N, such as NH_4^+, NO_3^- and amino acids (AA), are taken up by specialized transporters located on the fungal membrane in the extraradical mycelium. NH_3/NH_4^+ and P_i (the latter originated in AM fungi from the hydrolysis of polyphosphate) are imported from the symbiotic interface to the plant cells through selective transporters. Hexose transporters import plant-derived carbon to the fungus, whereas transporter proteins involved in the export of nutrients from either the plant or fungus have not been identified yet. This questions whether such processes indeed result from active, protein-mediated transport or involve passive export mechanisms.

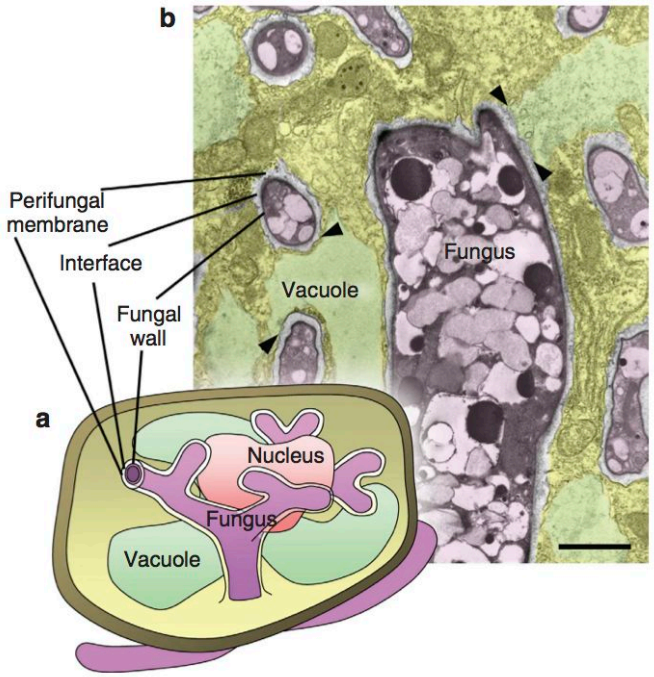

Figure 6 | The organization of an arbusculated cortical cell. The scheme in **a** shows how intracellular fungal hyphae are enveloped by the perifungal membrane, an extension of the host cell plasma membrane. This outlines the interface compartment, an apoplastic space that surrounds the fungus and mediates nutrient exchange. The central vacuole is resized into a smaller volume as the fungus develops to occupy most of the cell lumen. The nucleus enlarges and is positioned in the middle of the hyphal branches. The transmission electron image in **b** shows the details of the fungal accommodation process inside an arbusculated cell of carrot. The interface compartment (uncoloured) is clearly visible all around the fungus (pink), whereas plant organelles are observed all around the perifungal membrane. In particular, the tonoplast occasionally seems to be in direct connection (arrows) with the perifungal membrane (bar, 2 μm).

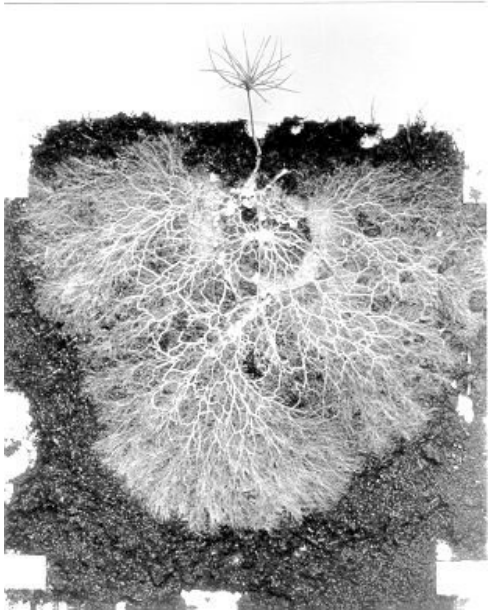

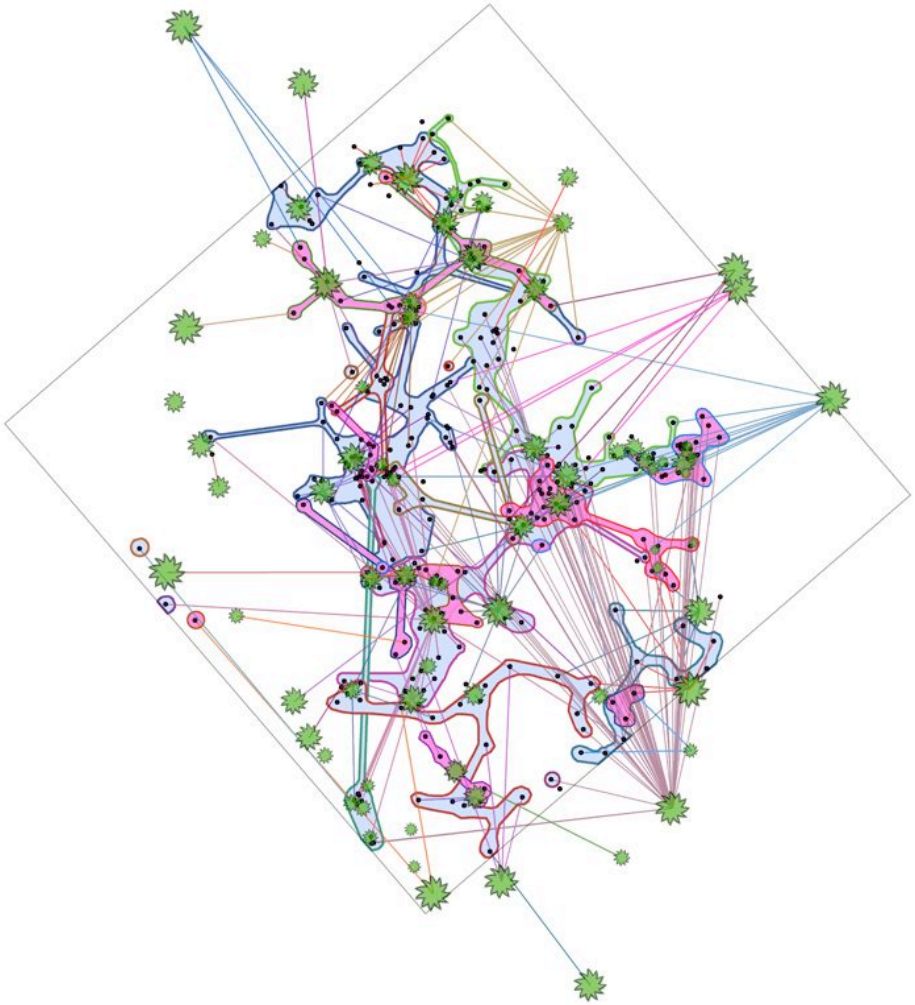

Reciprocal Rewards Stabilize Cooperation in the Mycorrhizal Symbiosis

E. Toby Kiers,[1]*† Marie Duhamel,[1,2] Yugandhar Beesetty,[3,4] Jerry A. Mensah,[4] Oscar Franken,[1] Erik Verbruggen,[1] Carl R. Fellbaum,[4] George A. Kowalchuk,[1,5] Miranda M. Hart,[6] Alberto Bago,[7]‡ Todd M. Palmer,[8] Stuart A. West,[9] Philippe Vandenkoornhuyse,[2] Jan Jansa,[10] Heike Bücking[4]†

Science 12 August 2011: vol. 333 no. 6044 880-882

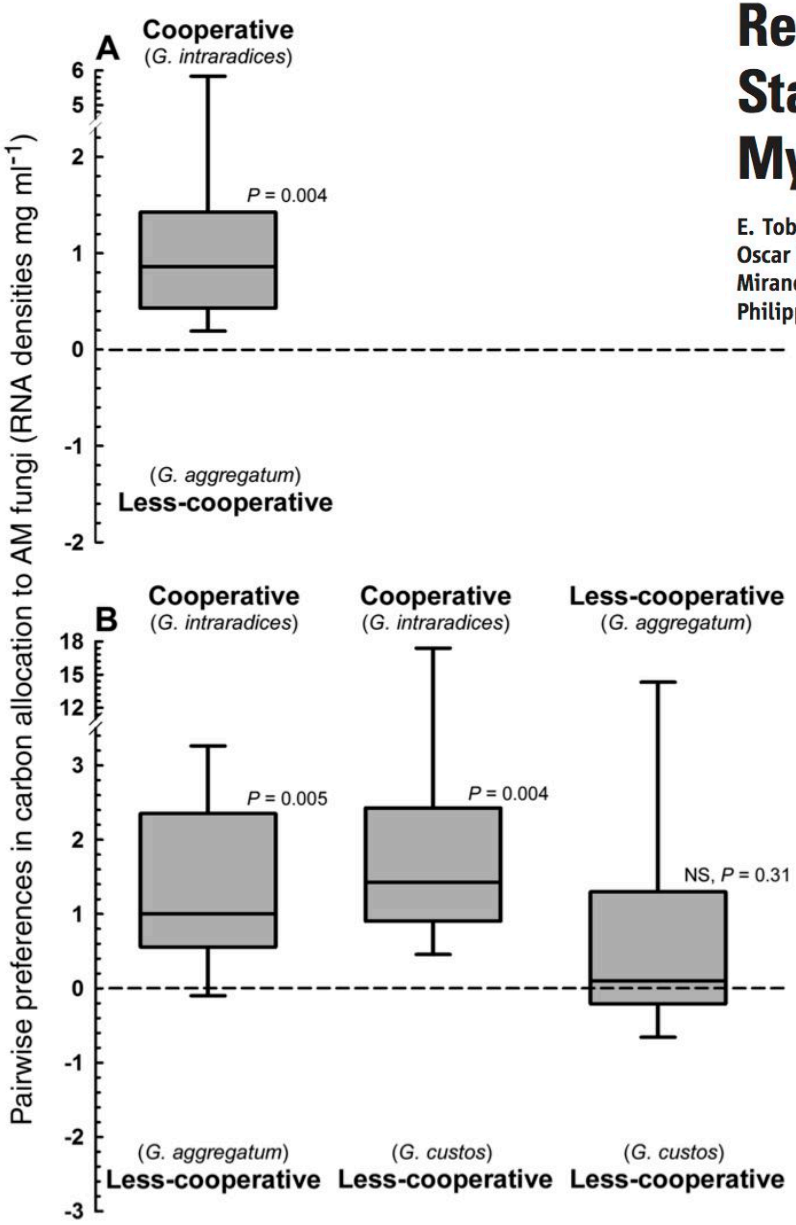

Fig. 1. Pair-wise comparisons of carbon allocation patterns to coexisting AM fungal species based on ^{13}C enrichment. Values above the zero line indicate preferential allocation to species above the line. (**A**) More carbon was allocated to the cooperative species (*G. intraradices*) compared with the less-cooperative species (*G. aggregatum*) in a two-species experiment. (**B**) When host plants were colonized with three AM fungal species, the RNA of the cooperative species (*G. intraradices*) was again significantly more enriched than that of the two less-cooperative species (*G. aggregatum* and *G. custos*). There was no significant difference in RNA enrichment between the two less-cooperative species. Data from all harvest times were pooled because there was no significant effect of time on RNA enrichment (Kruskal-Wallis, $P > 0.05$ for all three fungal species). Middle lines of box plots represent median values (n = 11), with bars showing value ranges (minimum to maximum). P values refer to nonparametric sign tests for differences of sample median from zero.

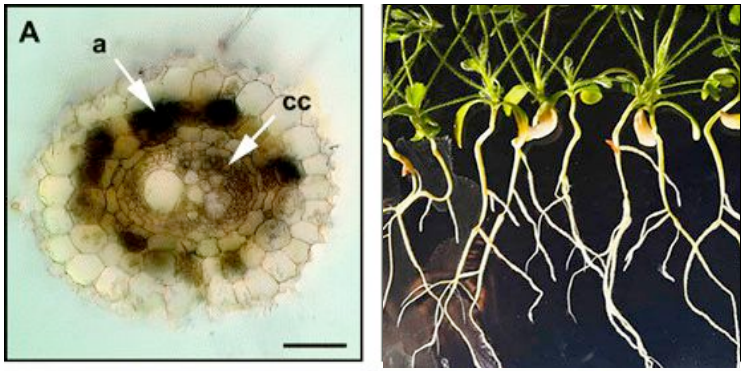

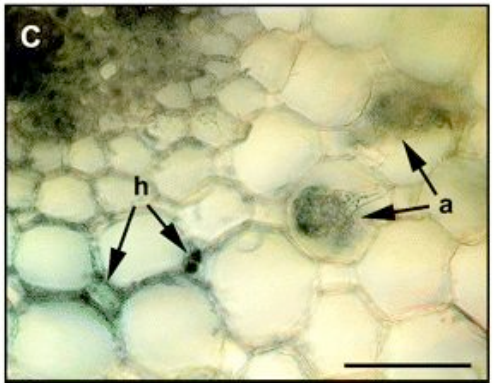

Medicago truncatula

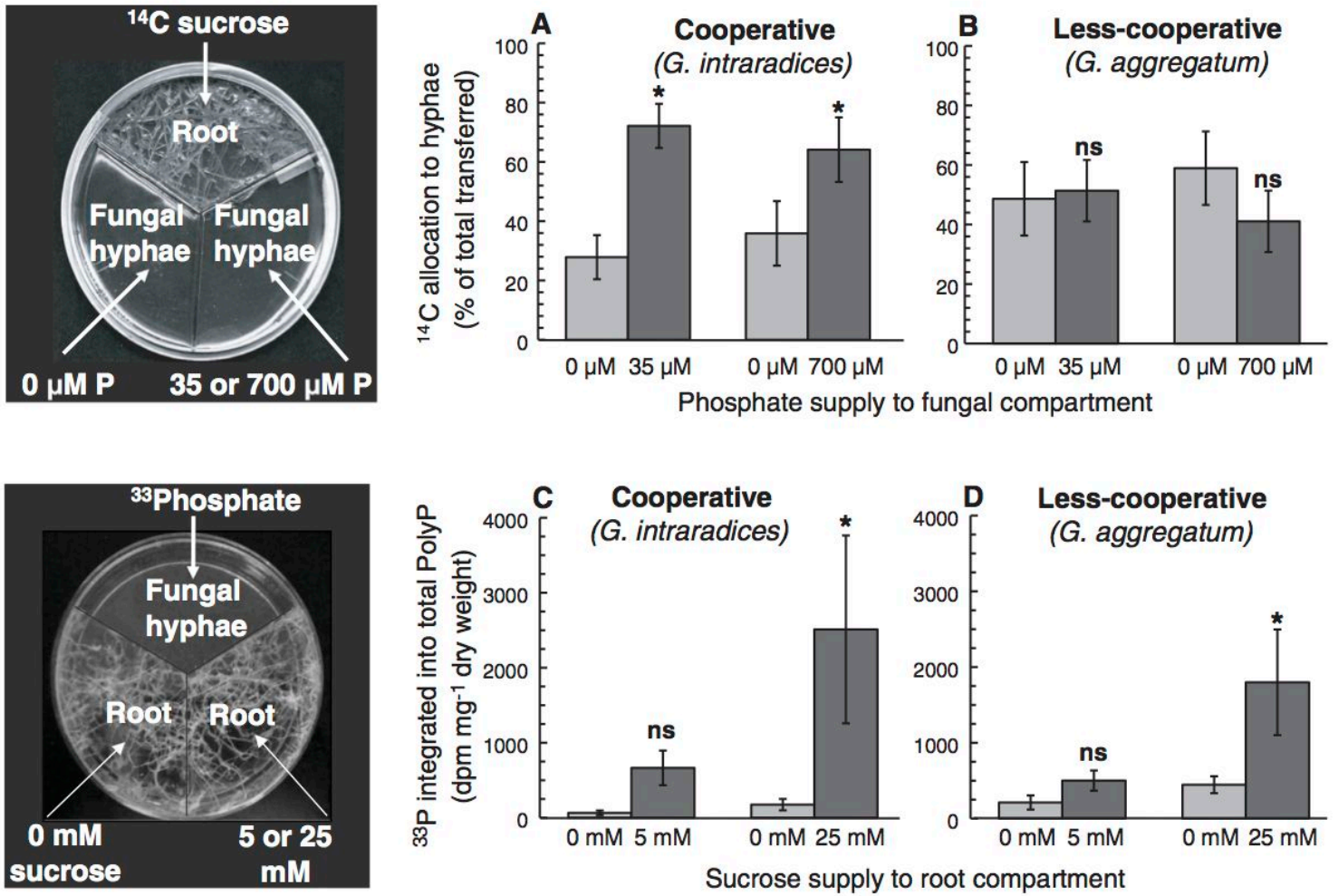

Fig. 2. Triple-plate experiments to mimic partner cooperation or defection. We found a significant effect of P availability on C allocation patterns ($F_{3,20} = 5.29$, $P = 0.0075$), with preferential allocation of C to the fungal compartments with access to more P in (**A**) *G. intraradices* but not in (**B**) *G. aggregatum*. In the reciprocal experiment, we found a significant effect of the C availability on P allocation patterns ($F_{7,58} = 7.298$, $P < 0.0001$), with a higher allocation of fungal P [measured as polyphosphate (PolyP)] to root compartments with higher C in both (**C**) *G. intraradices* and (**D**) *G. aggregatum*. However, the less-cooperative species *G. aggregatum*, remobilized a smaller percentage of its long-chained PolyP into short-chained PolyP, indicative of a hoarding strategy (figs. S6 and S8). Asterisks indicate significant differences between treatment means (Student-Newmans-Keuls test, $P \leq 0.05$). Error bars represent the means of 8 to 10 replicates ± 1 SEM.

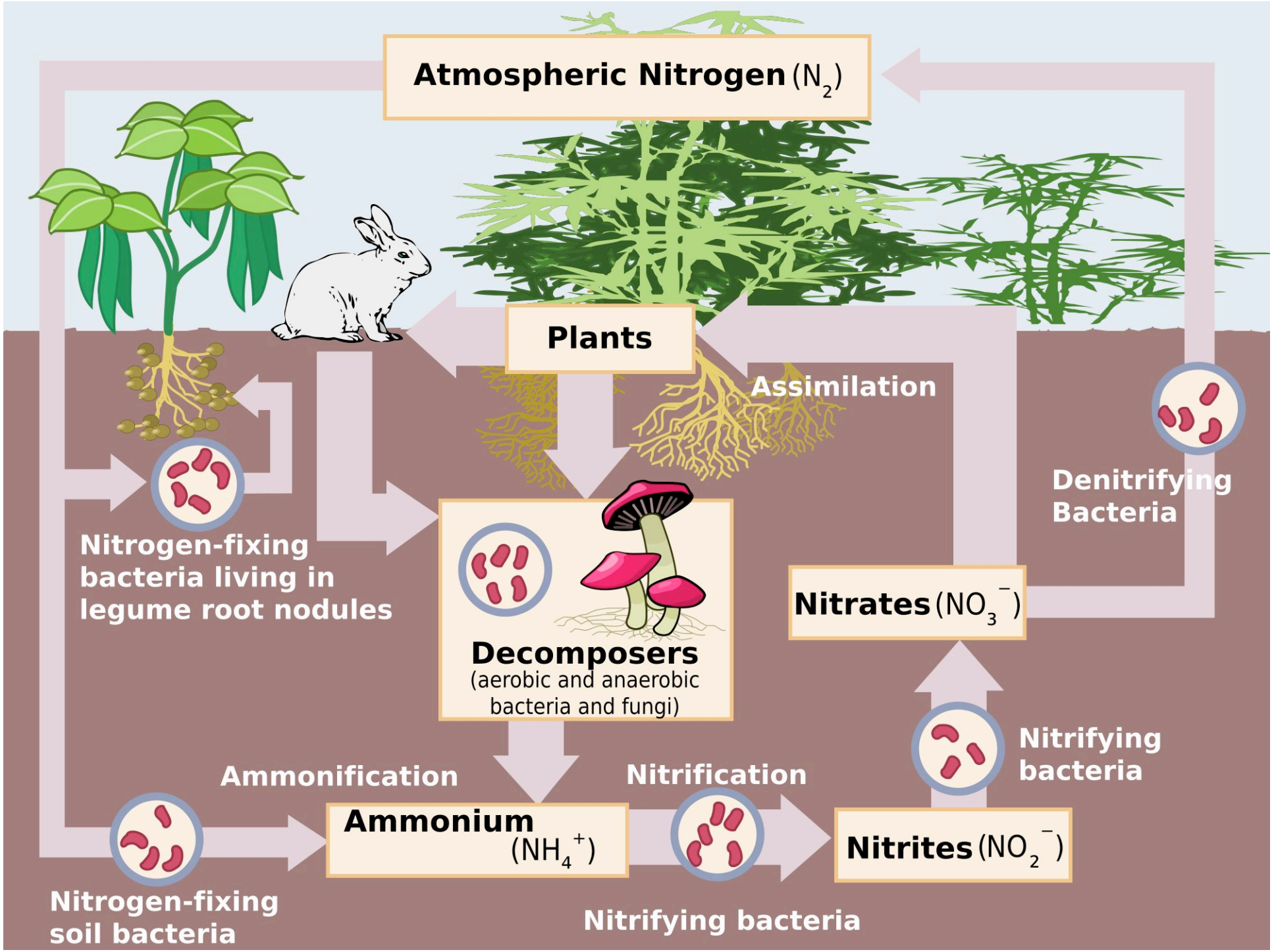
Atmospheric Nitrogen (N_2)
Plants
Assimilation
Denitrifying Bacteria
Nitrogen-fixing bacteria living in legume root nodules
Decomposers
(aerobic and anaerobic bacteria and fungi)
Nitrates (NO_3^-)
Nitrifying bacteria
Ammonification
Nitrification
Ammonium (NH_4^+)
Nitrites (NO_2^-)
Nitrogen-fixing soil bacteria
Nitrifying bacteria

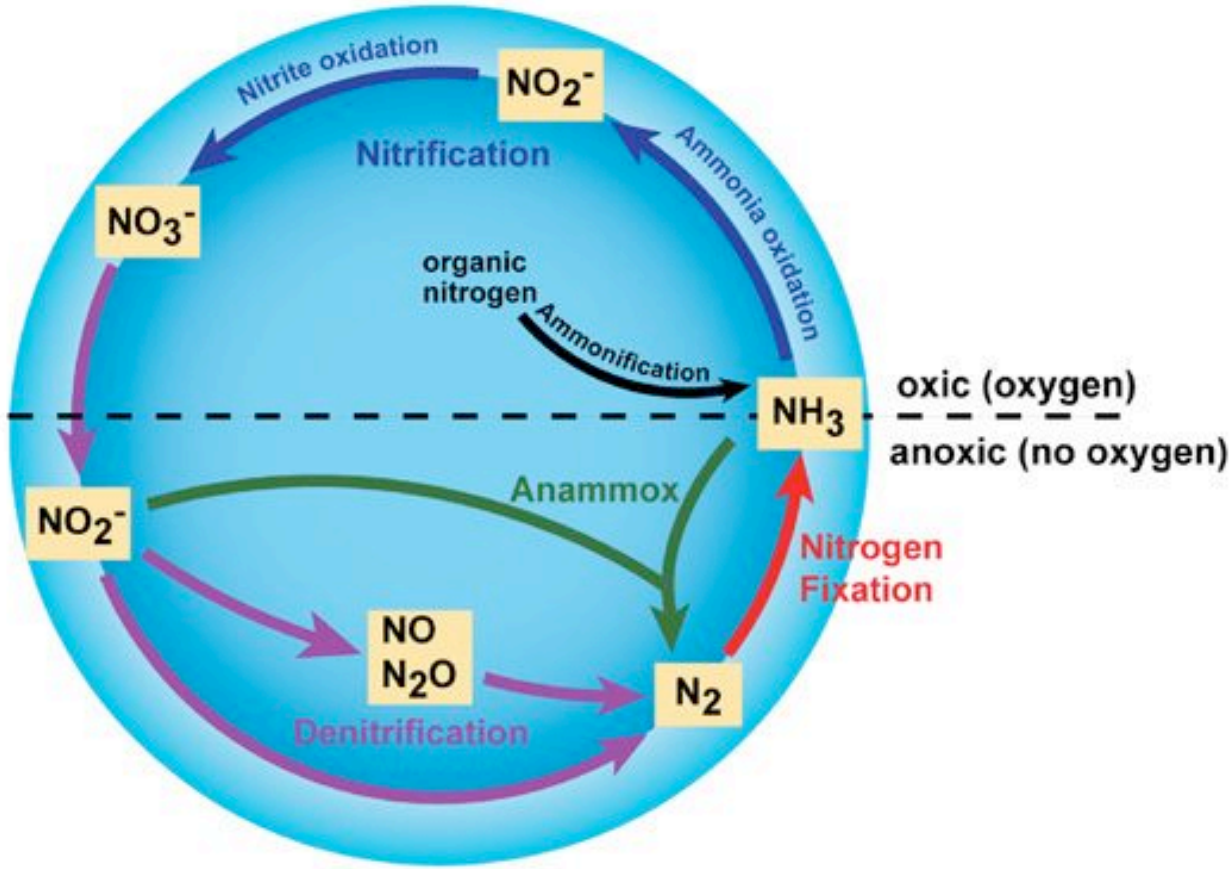
Nitrite oxidation
NO_2^-
Nitrification
Ammonia oxidation
NO_3^-
organic
nitrogen
Ammonification
NH_3
oxic (oxygen)
anoxic (no oxygen)
Anammox
NO_2^-
Nitrogen
Fixation
NO
N_2O
N_2
Denitrification

Units?

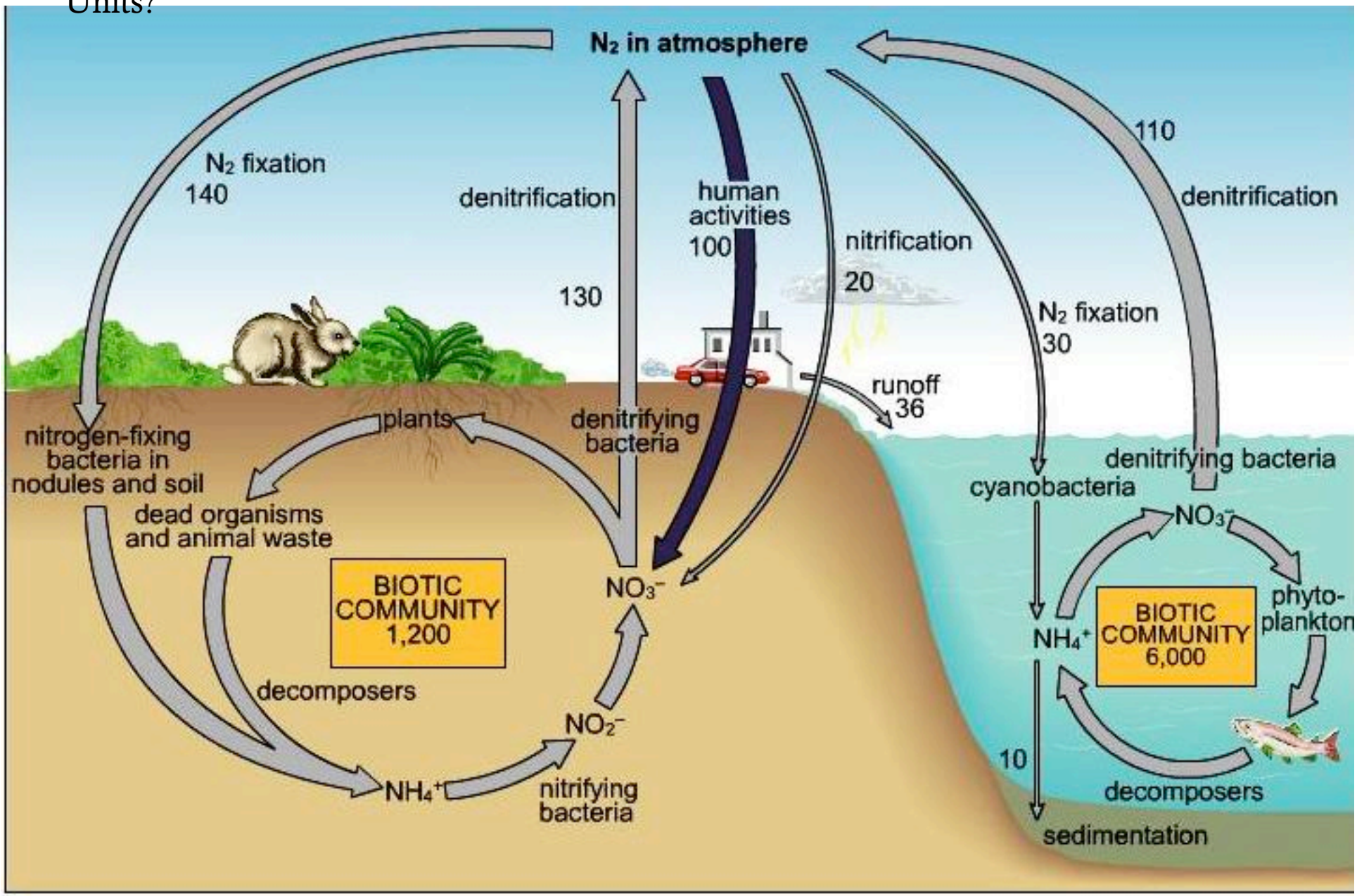
N_2 in atmosphere
N_2 fixation
140
denitrification
130
human activities
100
nitrification
20
N_2 fixation
30
110
denitrification
runoff
36
plants
denitrifying bacteria
nitrogen-fixing bacteria in nodules and soil
dead organisms and animal waste
BIOTIC COMMUNITY 1,200
NO_3^-
decomposers
NO_2^-
NH_4^+
nitrifying bacteria
denitrifying bacteria
cyanobacteria
NO_3^-
phyto-plankton
NH_4^+
BIOTIC COMMUNITY 6,000
10
decomposers
sedimentation

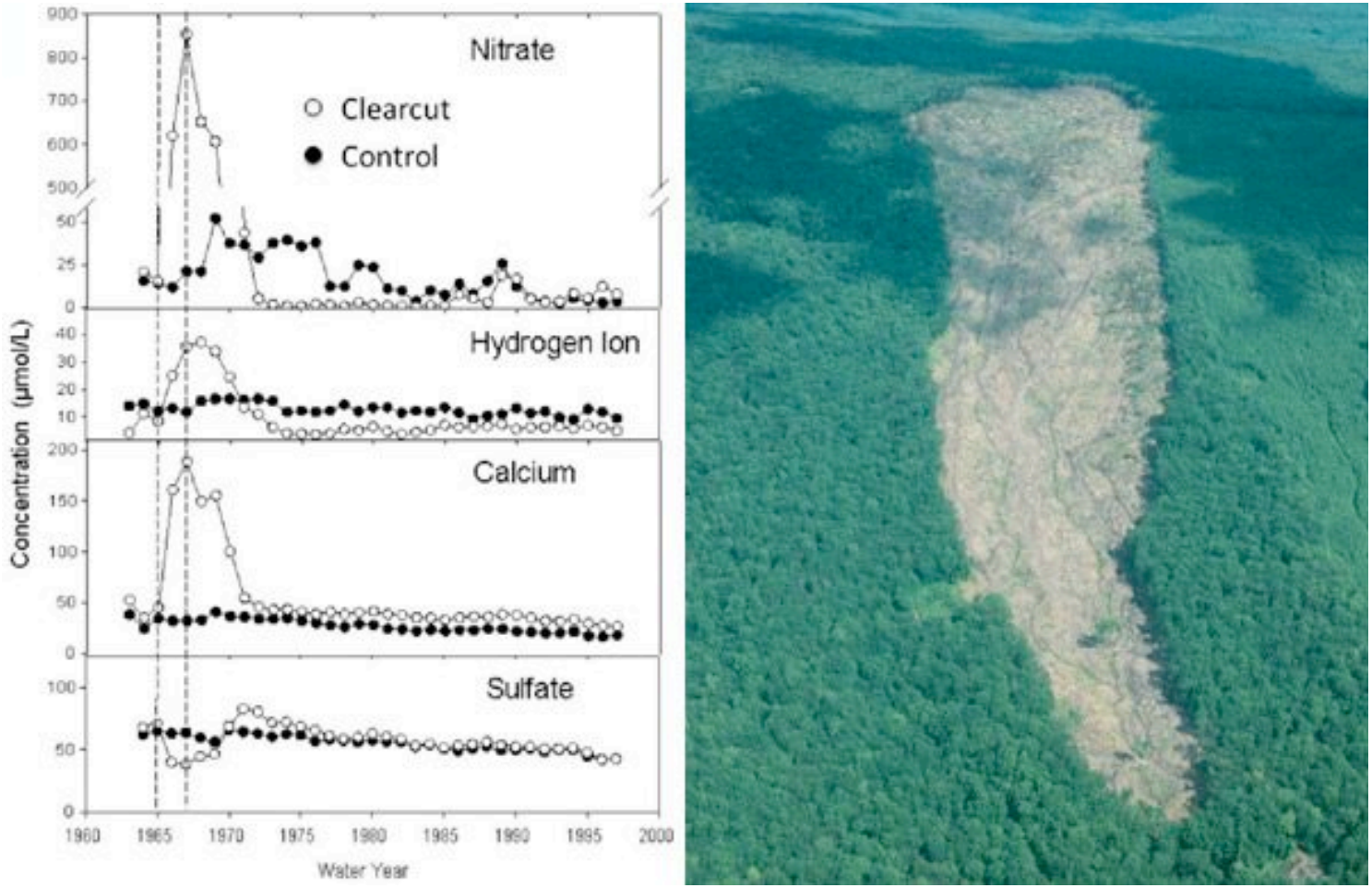

Figure 8: An experimental reference watershed at the Hubbard Brook Experimental Forest in the White Mountains of New Hampshire, USA

Researchers have manipulated entire watersheds, for example by whole-tree harvesting, and then monitored losses of various elements. The whole-tree harvesting of watershed 2 in 1965 affected the uptake and loss of nutrients and elements within the forest ecosystem and was followed by high loss rates of nitrate, hydrogen ions, and calcium ions in stream waters for several years. (Stream chemistry data were provided by G. E. Likens with funding from the National Science Foundation and The A. W. Mellon Foundation.)

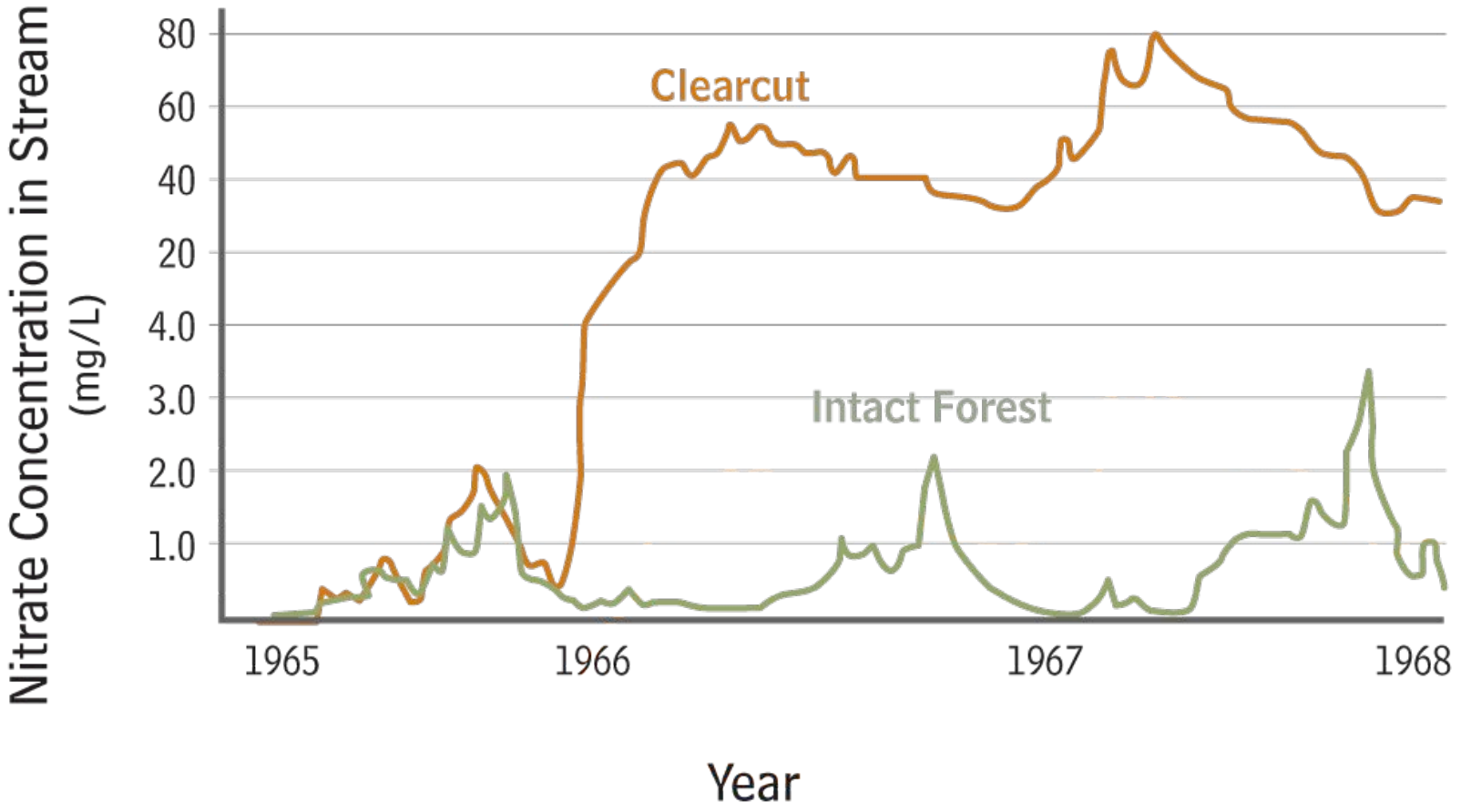

Nitrogen concentration in streams flowing from adjacent clearcut and intact forests at Hubbard Brook, NH (after Likens et al., 1970).

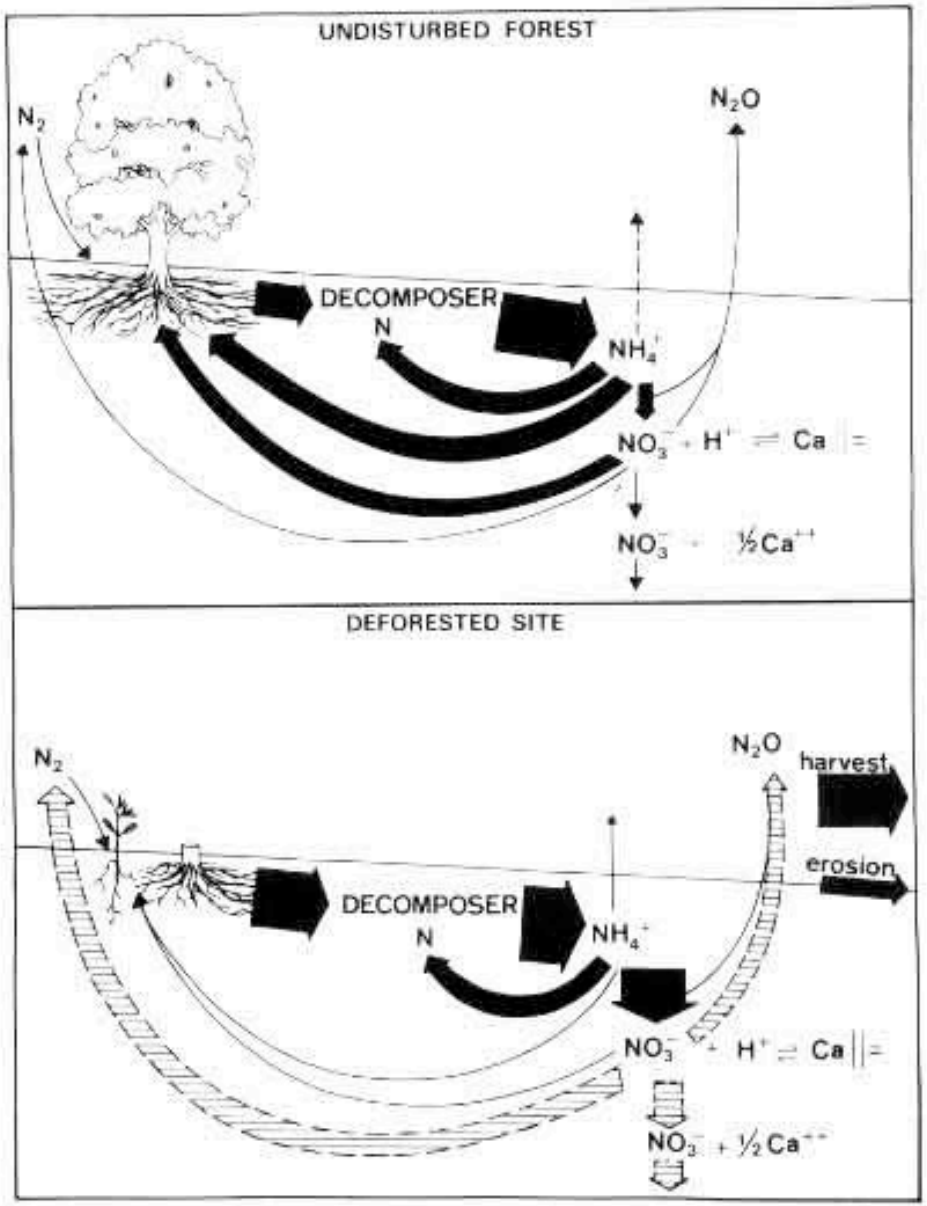

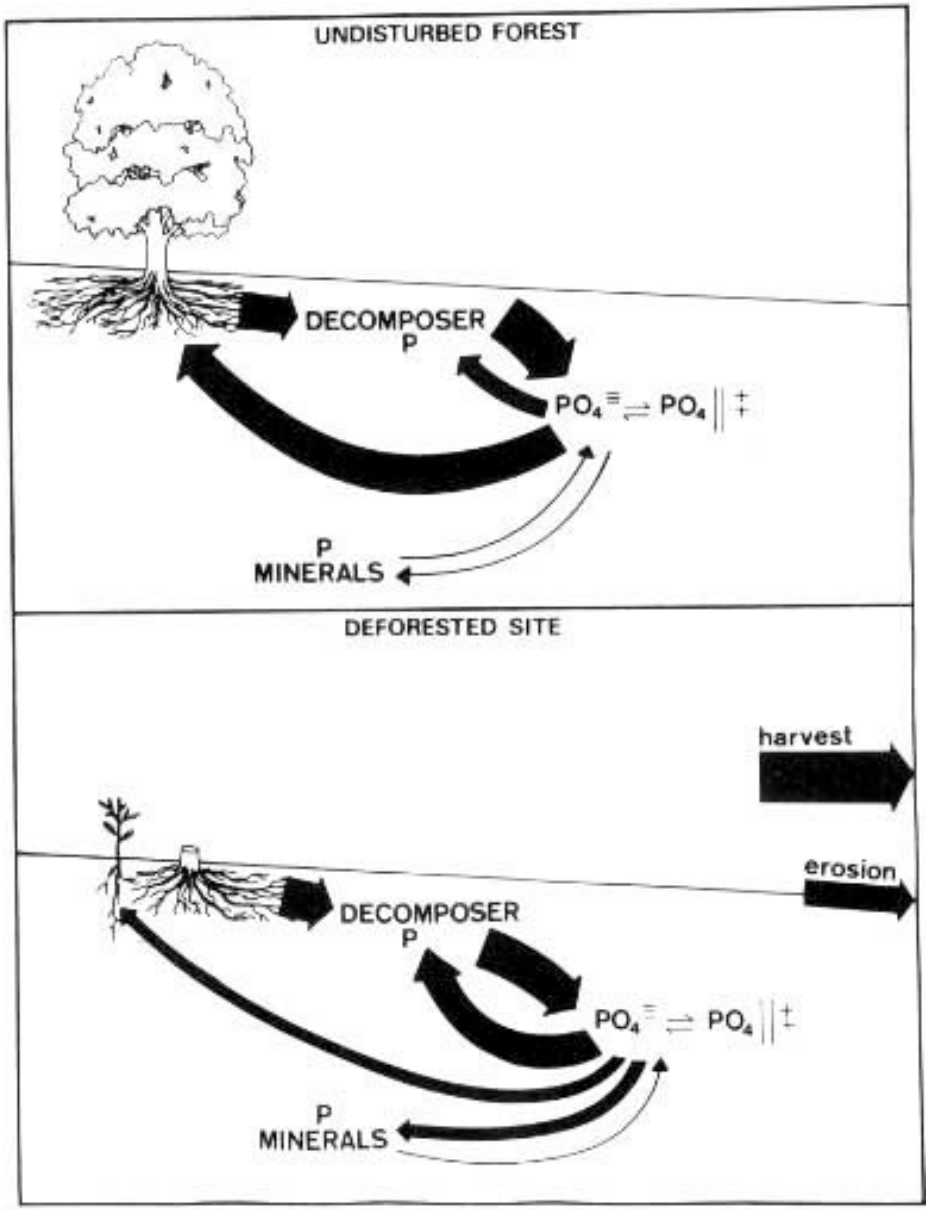

http://www.scopenvironment.org/downloadpubs/scope21/chapter07.html

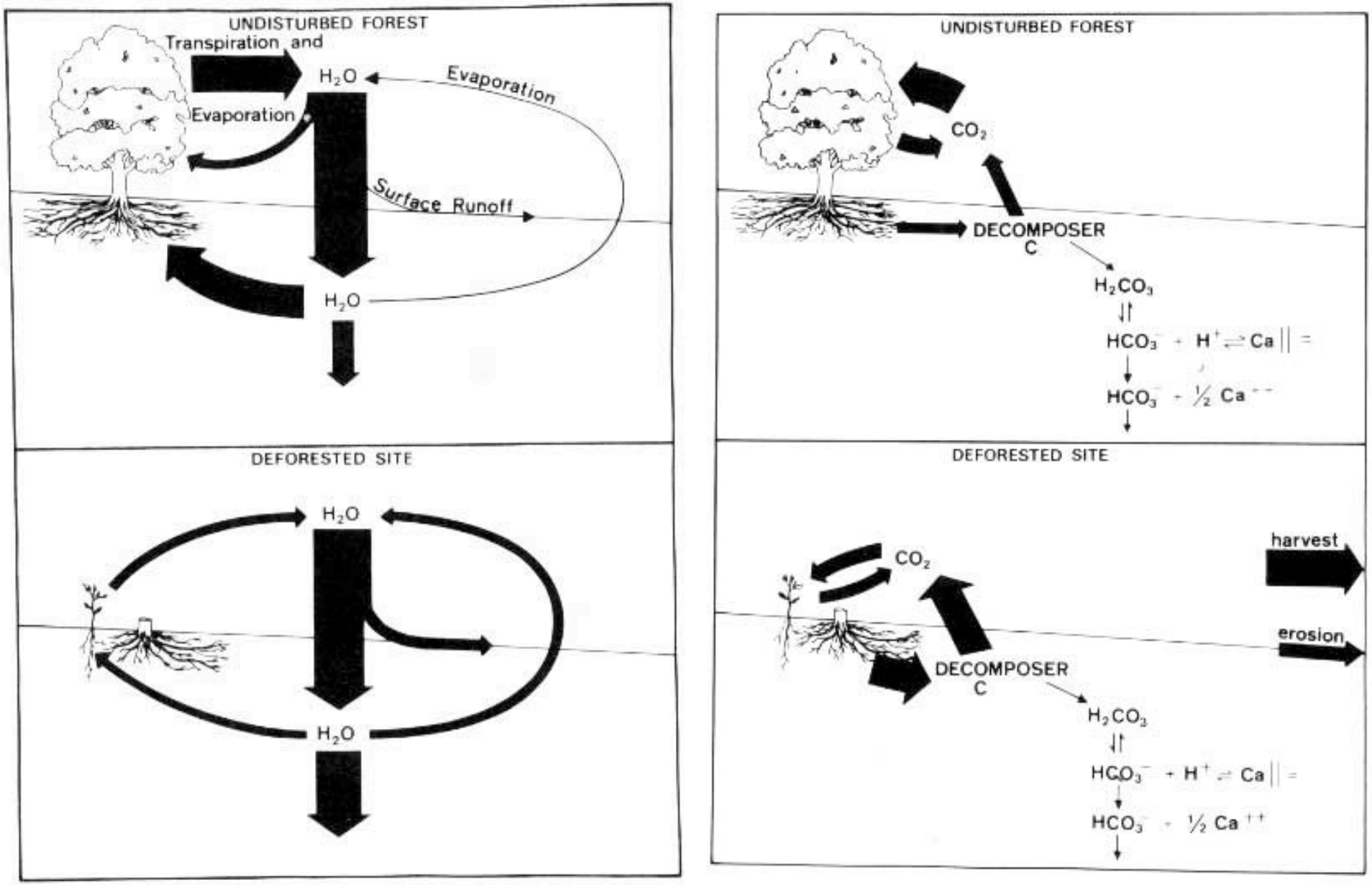

http://www.scopenvironment.org/downloadpubs/scope21/chapter07.html

Haber (or Haber-Bosch) process

$N_2 + 3\ H_2 \rightleftharpoons 2\ NH_3$

$(\Delta H = -92.22\ kJ/mol)$

…and the Green Revolution


Fritz Haber

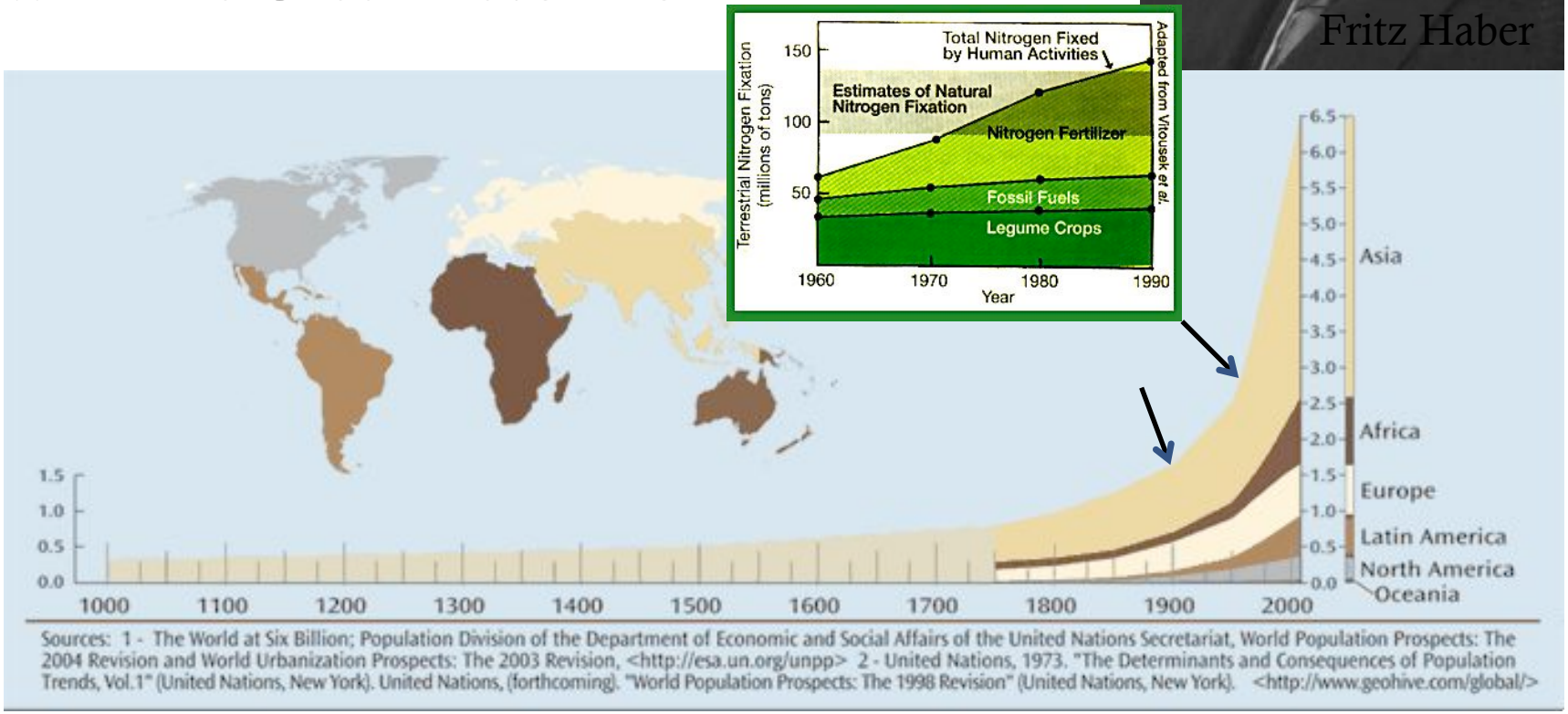

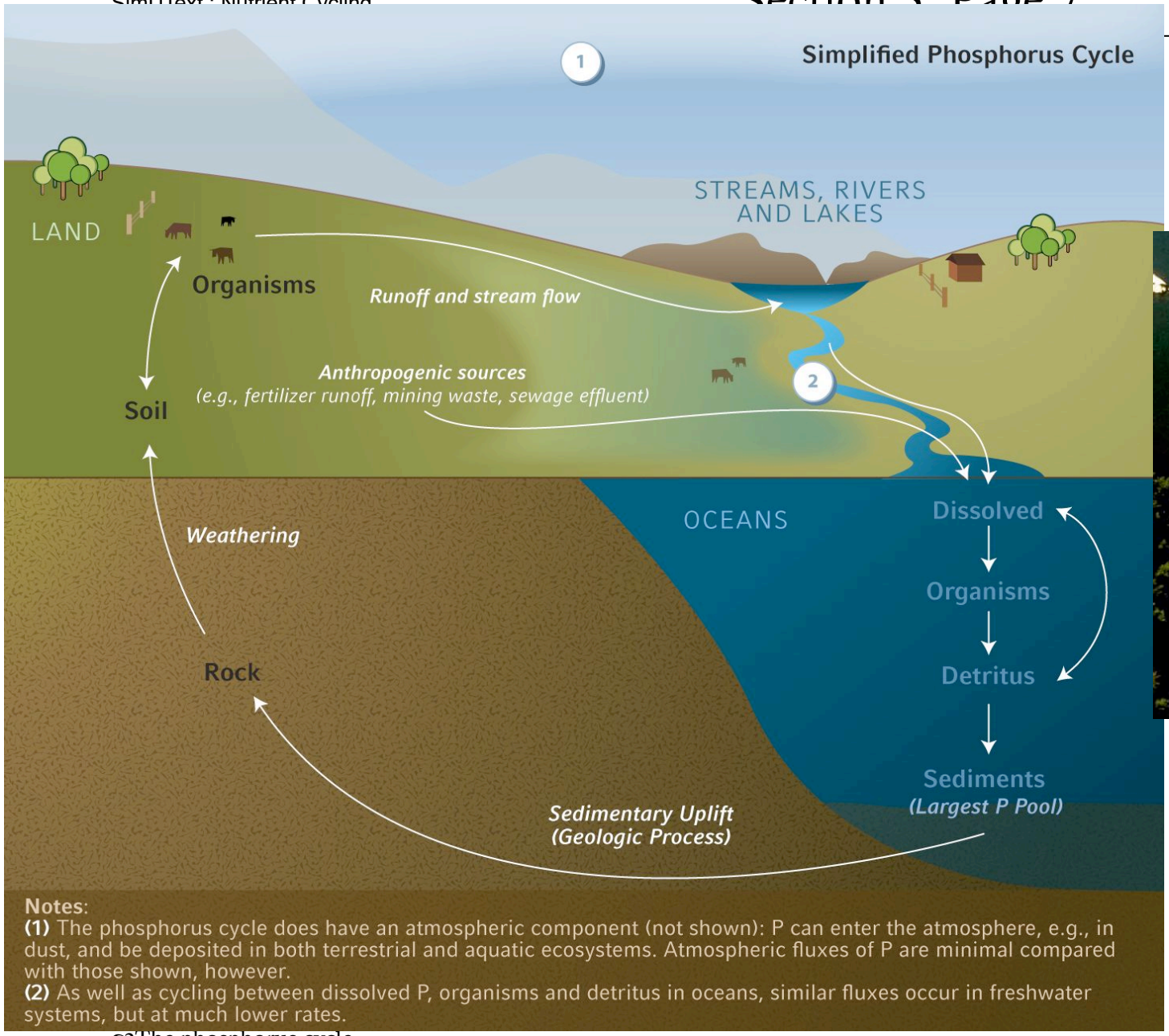

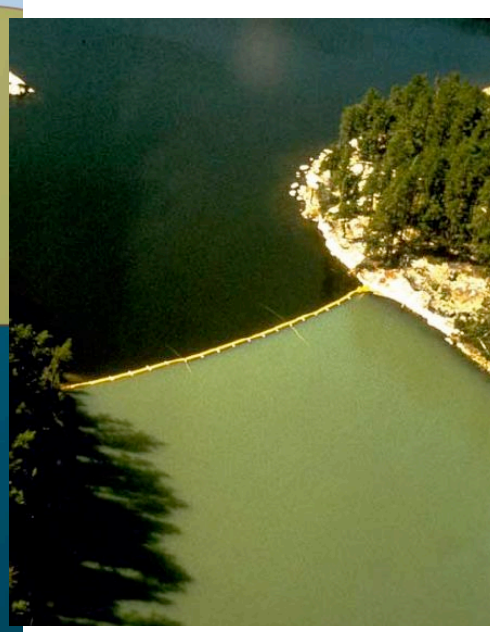

☙The phosphorus cycle.

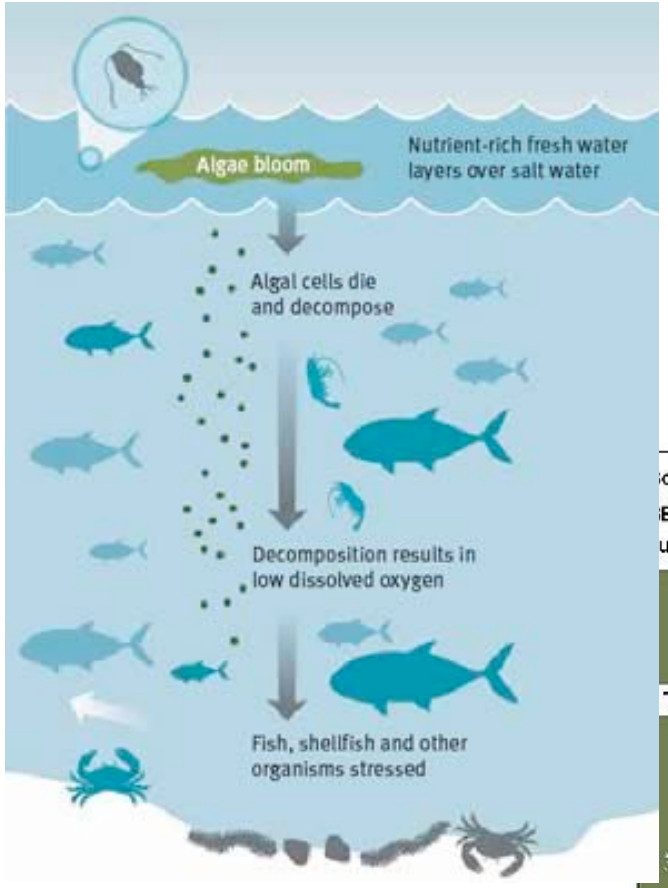
Algae bloom
Nutrient-rich fresh water layers over salt water
Algal cells die and decompose
Decomposition results in low dissolved oxygen
Fish, shellfish and other organisms stressed

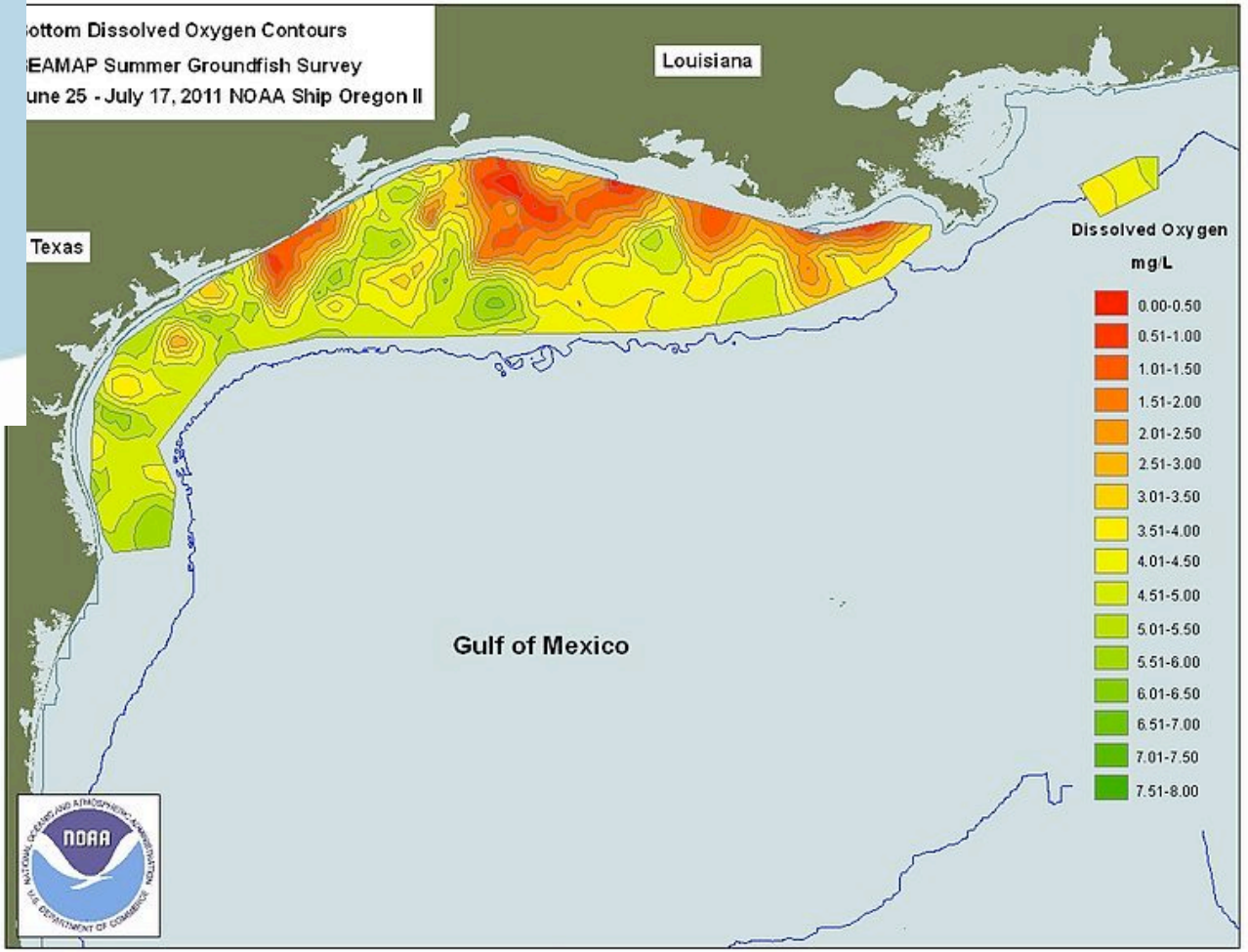
ottom Dissolved Oxygen Contours
EAMAP Summer Groundfish Survey
une 25 - July 17, 2011 NOAA Ship Oregon II
Louisiana
Texas
Gulf of Mexico
Dissolved Oxygen
mg/L
0.00-0.50
0.51-1.00
1.01-1.50
1.51-2.00
2.01-2.50
2.51-3.00
3.01-3.50
3.51-4.00
4.01-4.50
4.51-5.00
5.01-5.50
5.51-6.00
6.01-6.50
6.51-7.00
7.01-7.50
7.51-8.00
NOAA

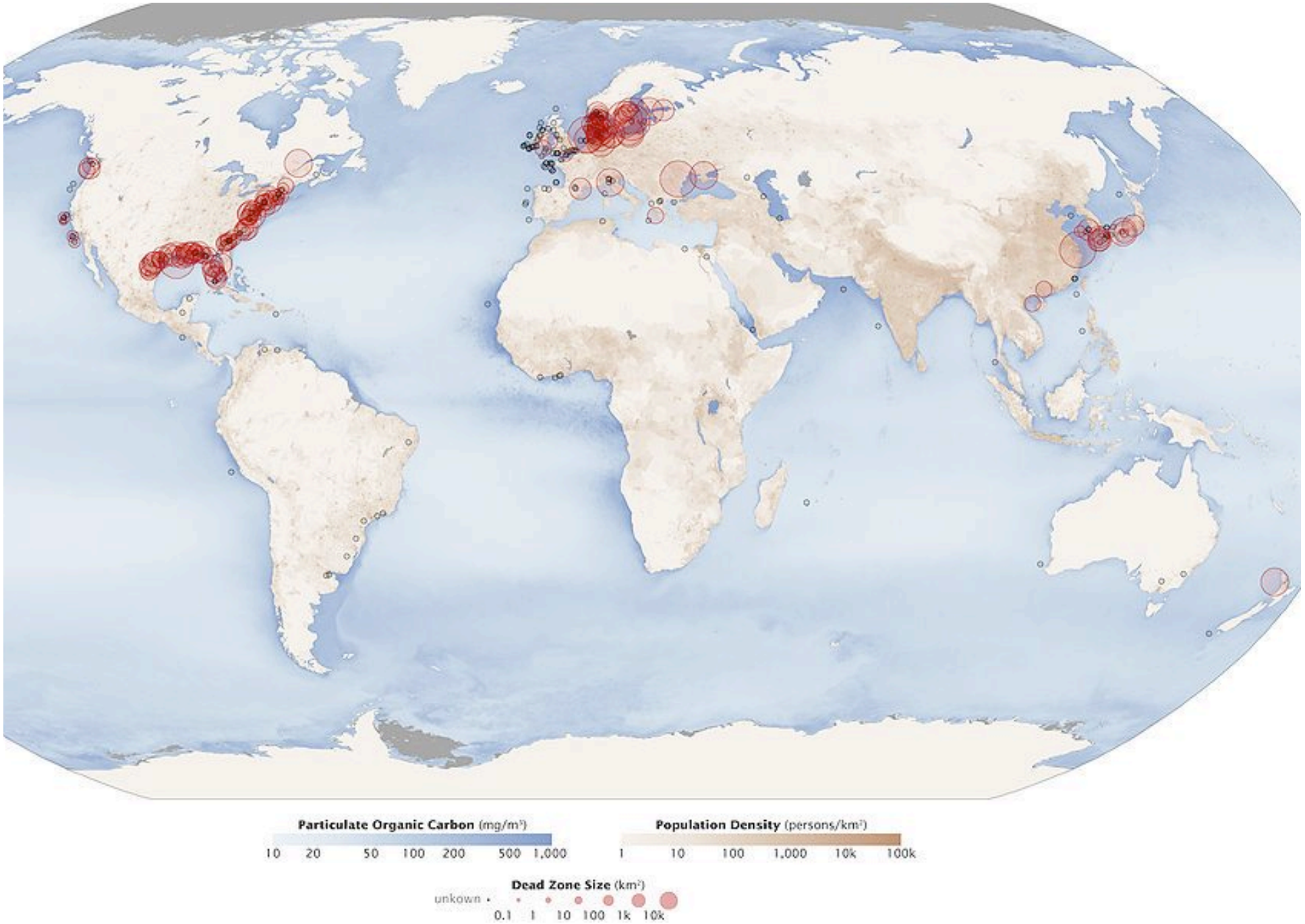

http://en.wikipedia.org/wiki/File:Aquatic_Dead_Zones.jpg

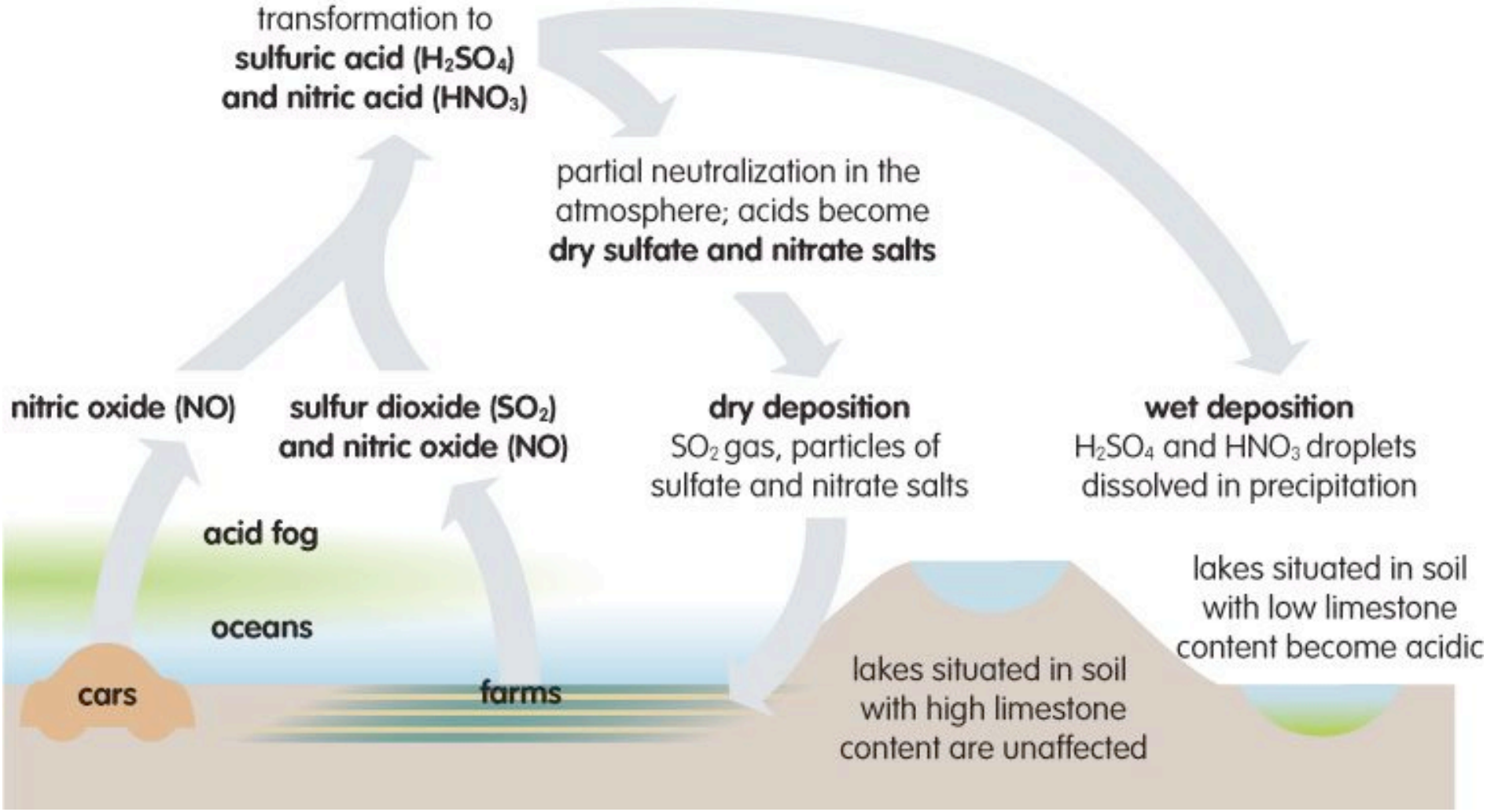

http://sparkcharts.sparknotes.com/gensci/envsci/section4.php

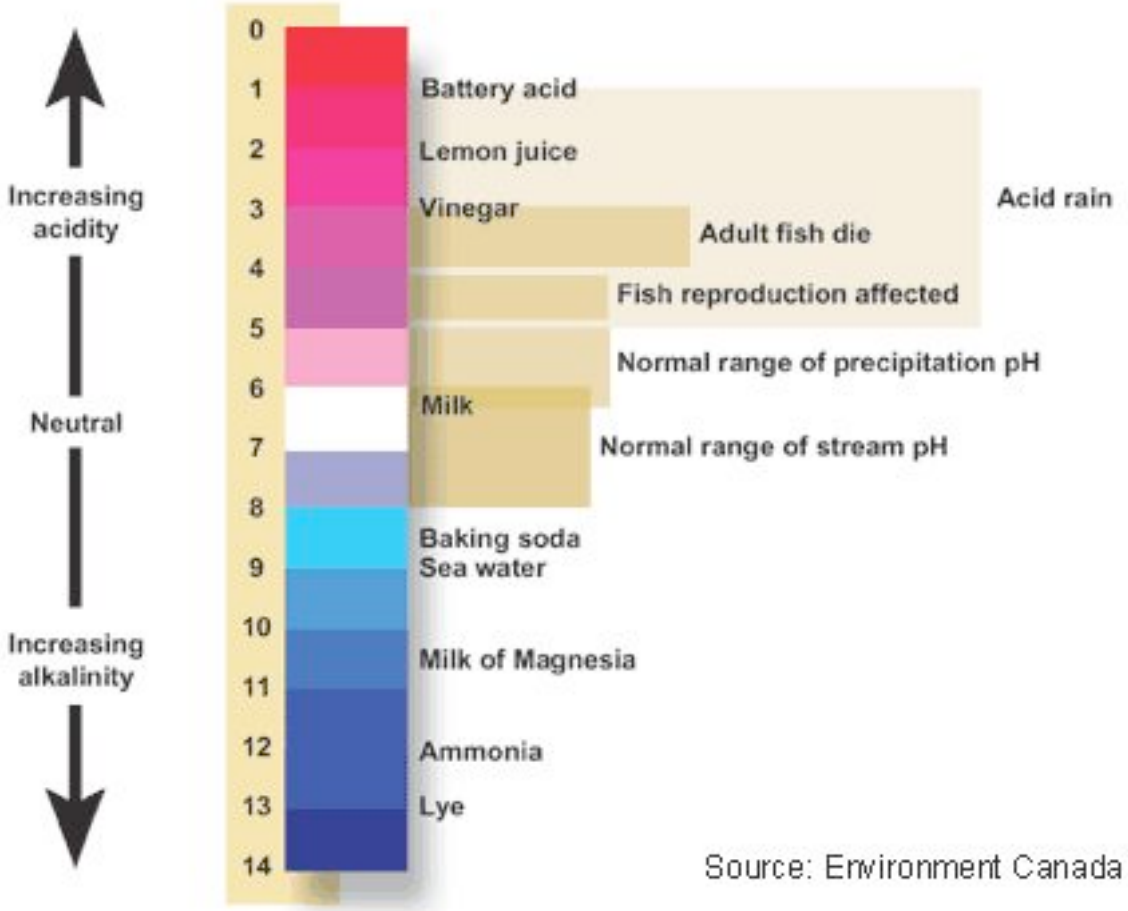

http://ga.water.usgs.gov/edu/ph.html

Hydrogen ion concentration as pH of precipitation, 2002

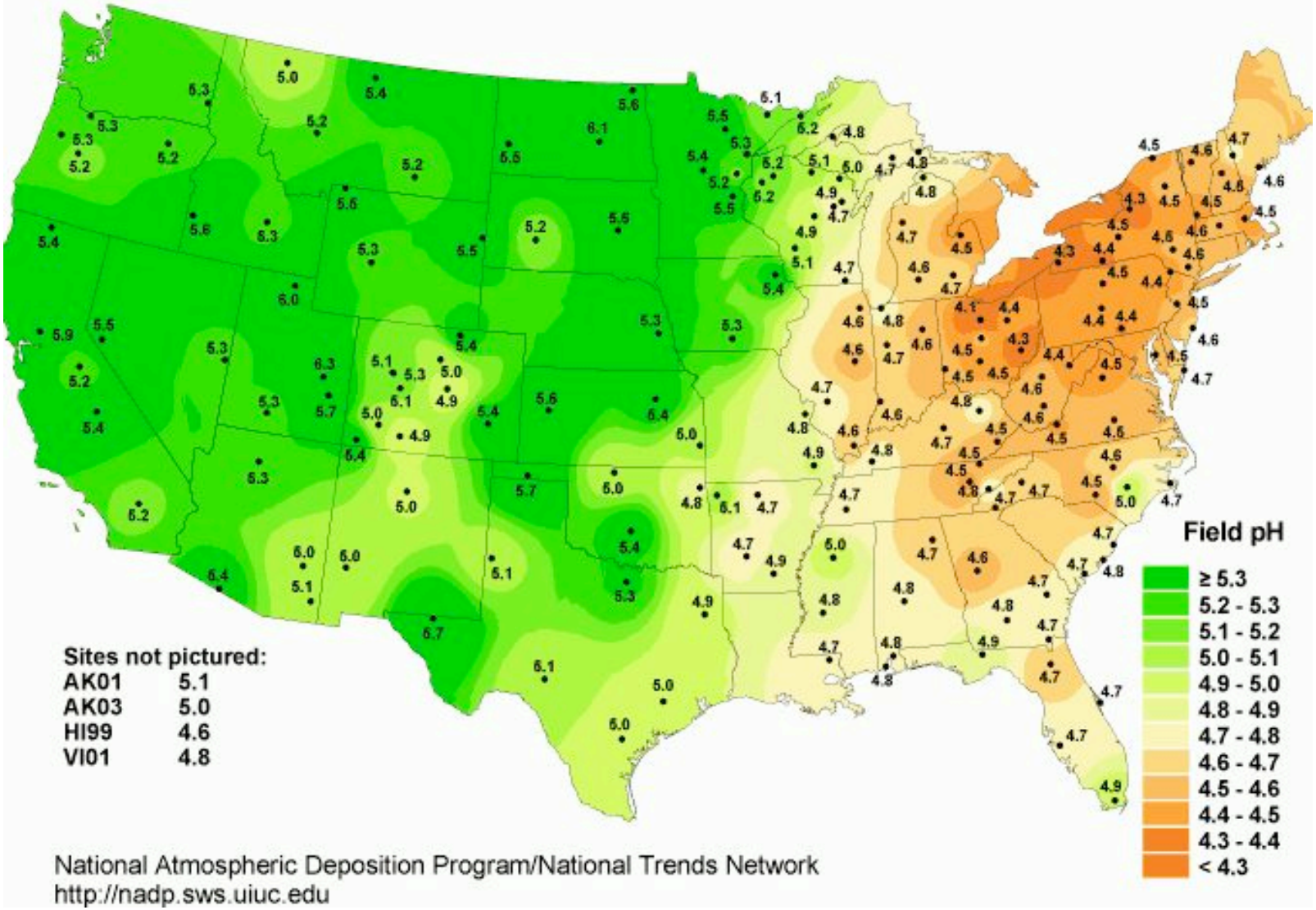

National Atmospheric Deposition Program/National Trends Network
http://nadp.sws.uiuc.edu

Hydrogen ion concentration as pH from measurements made at the Central Analytical Laboratory, 2010

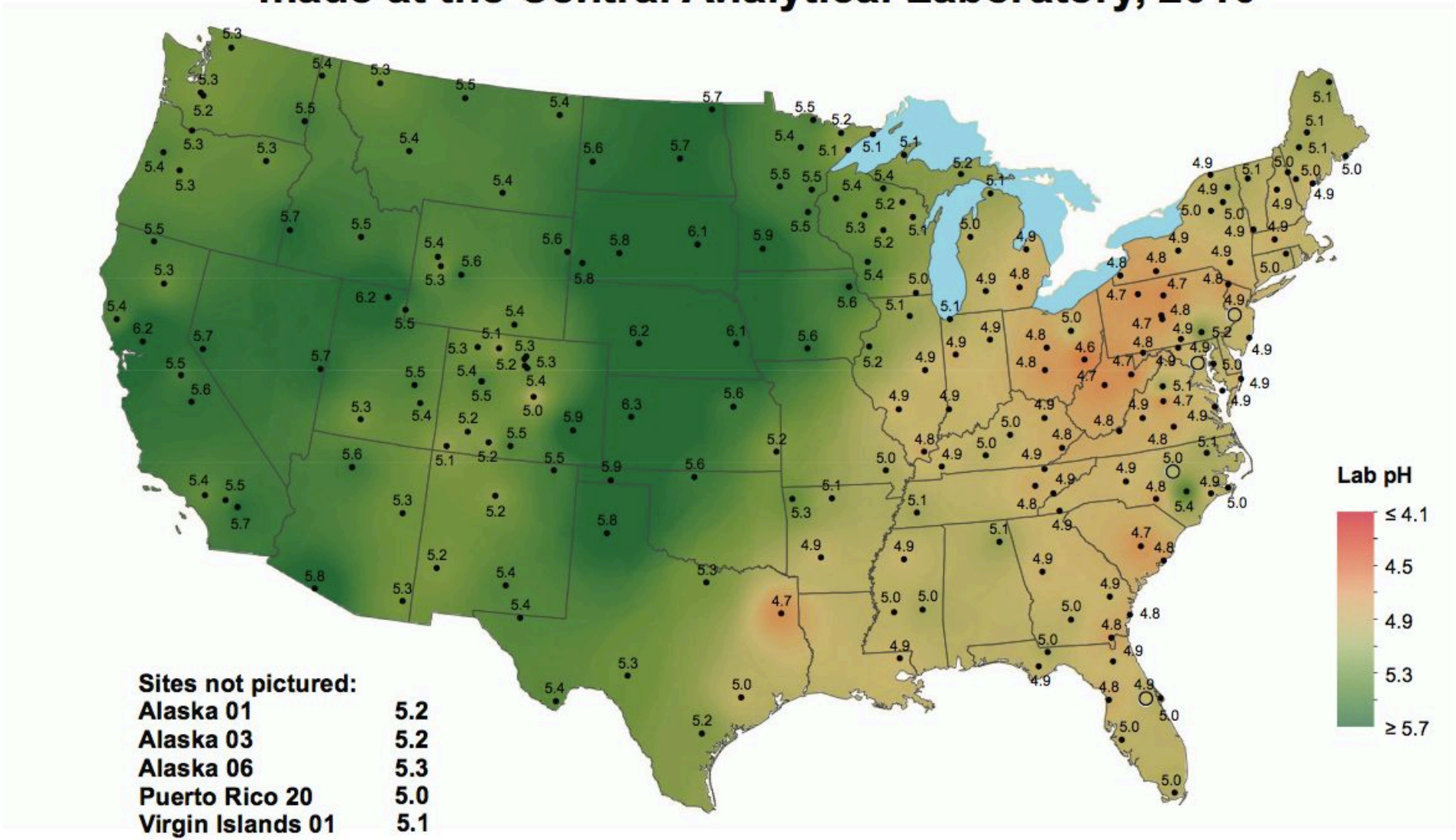

National Atmospheric Deposition Program/National Trends Network
http://nadp.isws.illinois.edu

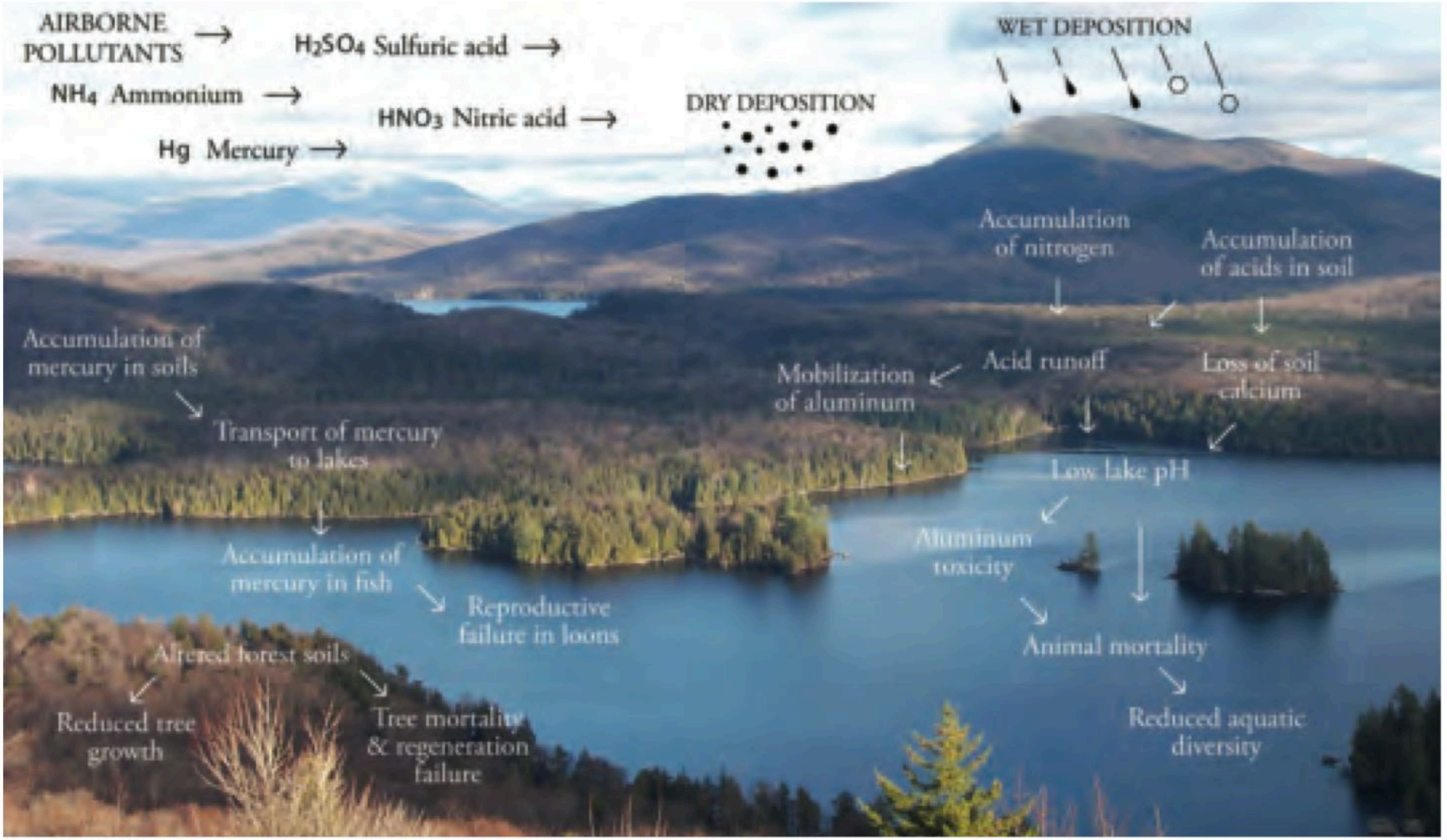

The multiple ecological pathways and impacts of acid deposition and mercury in forested watersheds in the Eastern U.S.
(Courtesy of the Adirondack Nature Conservancy and Adirondack Land Trust - photograph by Bill Brown; conceptual diagram by Jerry Jenkins).

Lovett, G.M., and T.H. Tear. 2008. Threats from Above: Air Pollution Impacts on Ecosystems and Biological Diversity in the Eastern United States. The Nature Conservancy and the Cary Institute of Ecosystem Studies.

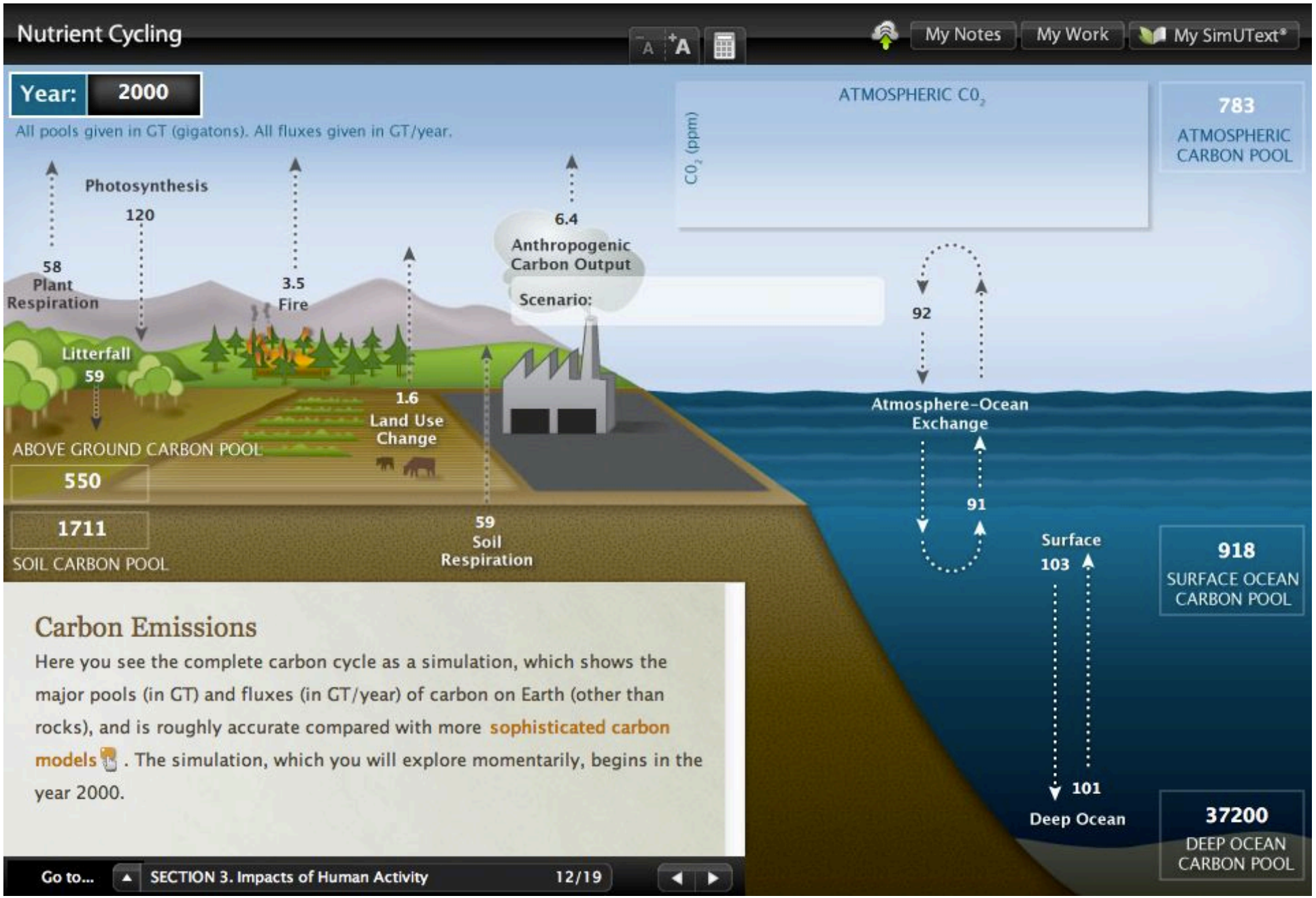
Nutrient Cycling
My Notes
My Work
My SimUText®
Year: 2000
All pools given in GT (gigatons). All fluxes given in GT/year.
ATMOSPHERIC CO_2
CO_2 (ppm)
783
ATMOSPHERIC CARBON POOL
Photosynthesis
120
58
Plant Respiration
3.5
Fire
6.4
Anthropogenic Carbon Output
Scenario:
92
Litterfall
59
1.6
Land Use Change
Atmosphere-Ocean Exchange
91
ABOVE GROUND CARBON POOL
550
1711
SOIL CARBON POOL
59
Soil Respiration
Surface
103
101
Deep Ocean
918
SURFACE OCEAN CARBON POOL
37200
DEEP OCEAN CARBON POOL
Carbon Emissions
Here you see the complete carbon cycle as a simulation, which shows the major pools (in GT) and fluxes (in GT/year) of carbon on Earth (other than rocks), and is roughly accurate compared with more sophisticated carbon models . The simulation, which you will explore momentarily, begins in the year 2000.
Go to...
SECTION 3. Impacts of Human Activity
12/19

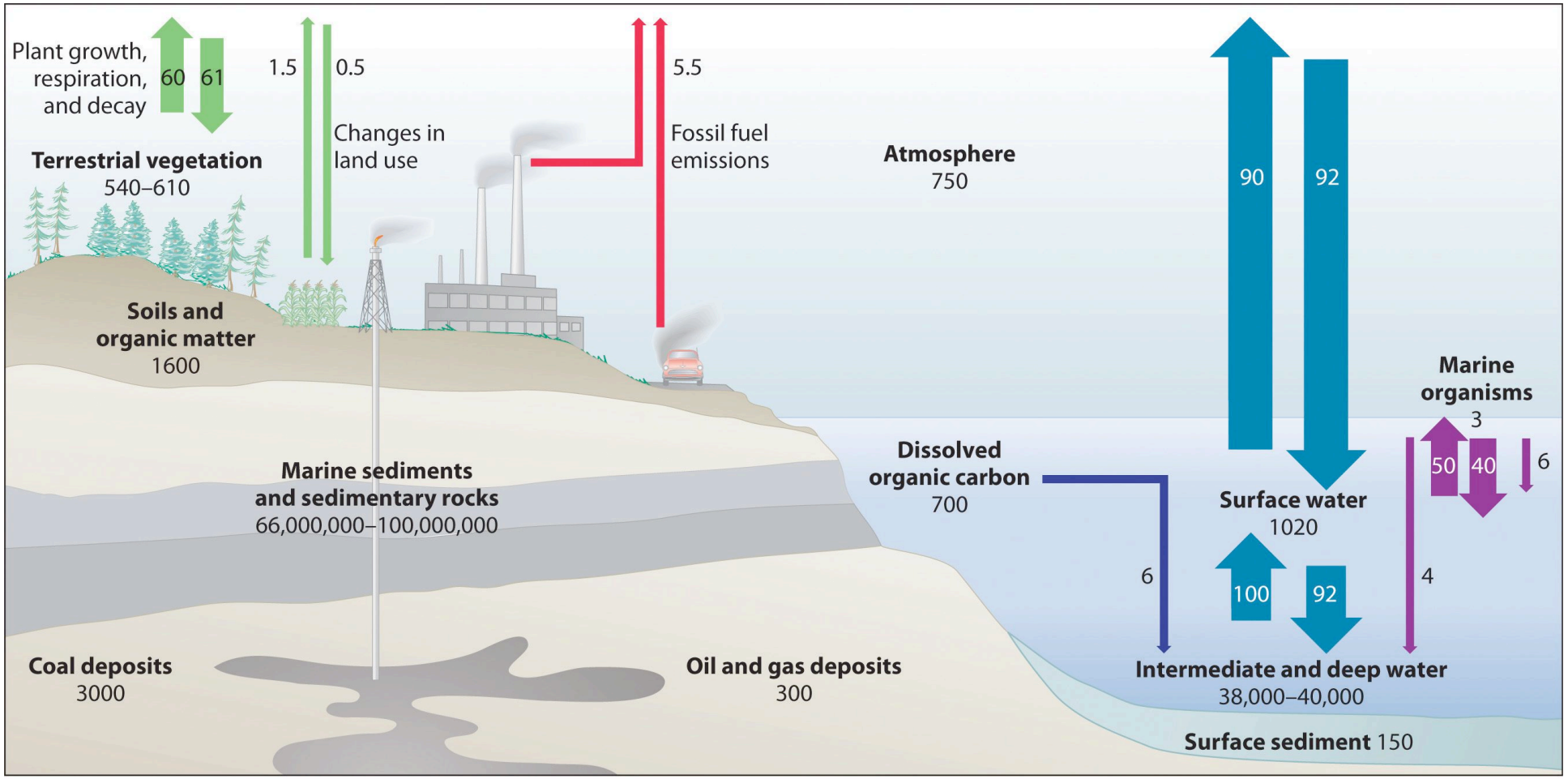

Volumes and exchanges in billions of metric tons

General Chemistry: Principles, Patterns, and Applications, v. 1.0
by Bruce Averill and Patricia Eldredge

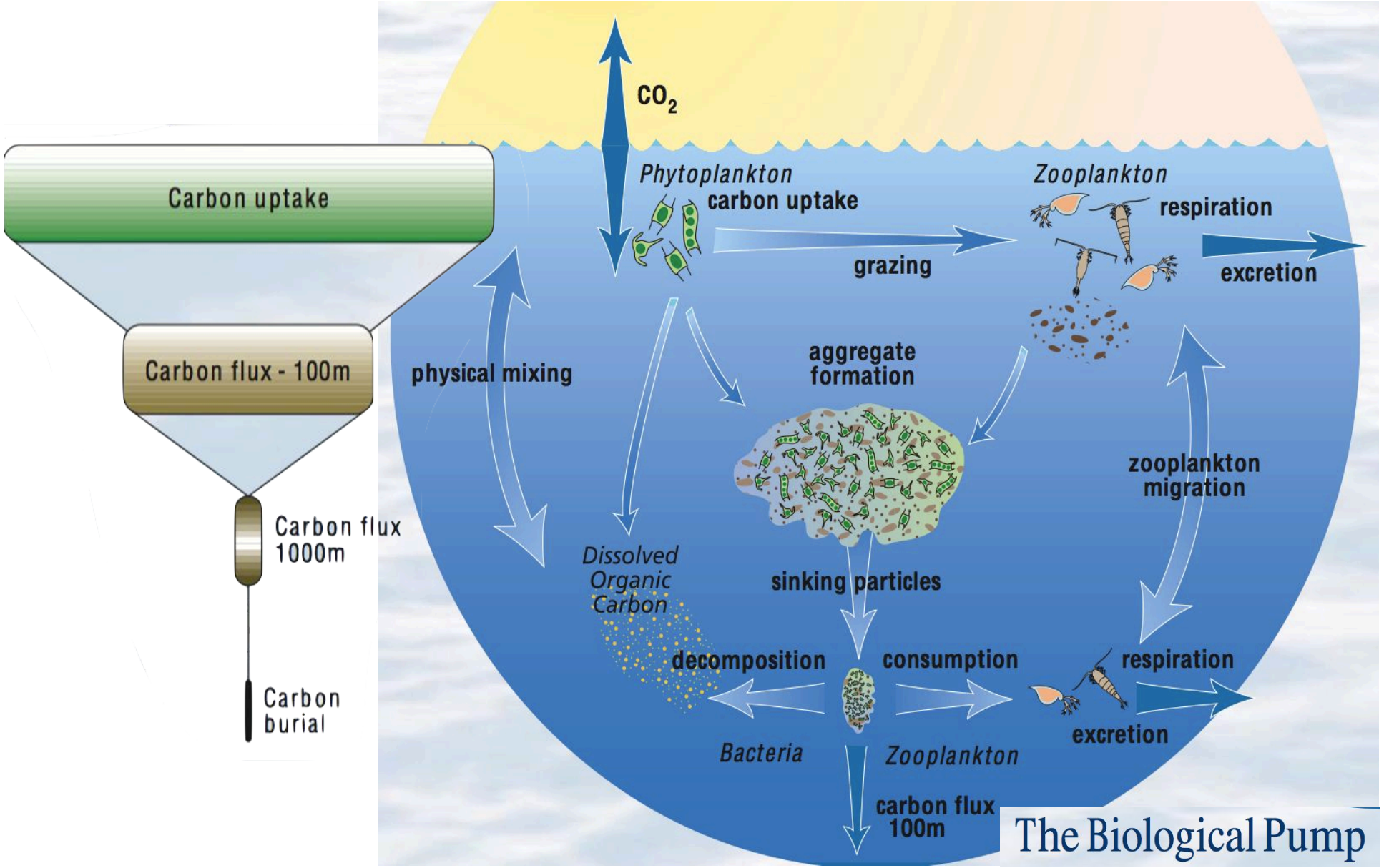
Carbon uptake
Carbon flux - 100m
Carbon flux 1000m
Carbon burial
CO_2
Phytoplankton
carbon uptake
Zooplankton
respiration
grazing
excretion
physical mixing
aggregate formation
zooplankton migration
Dissolved Organic Carbon
sinking particles
decomposition
consumption
respiration
excretion
Bacteria
Zooplankton
carbon flux 100m
The Biological Pump
U.S. Joint Global Ocean Flux Study

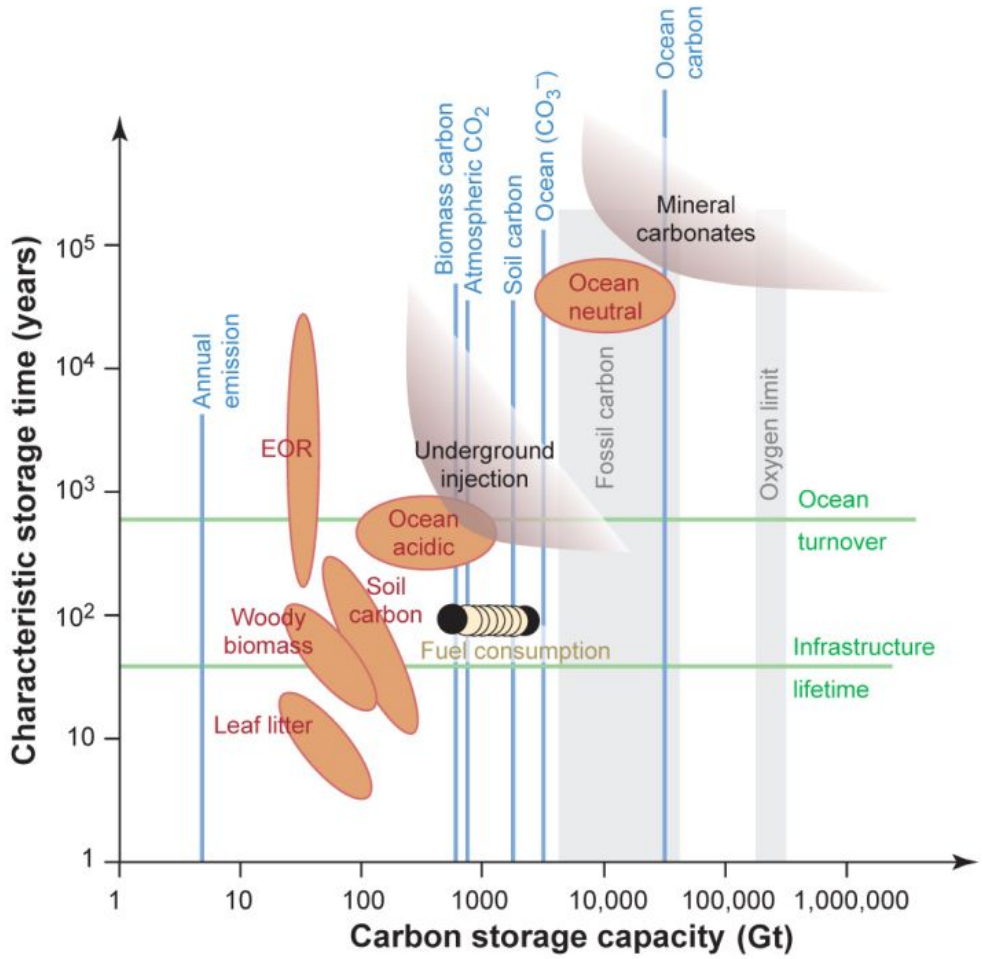

Estimated storage capacities and times for various sequestration methods. The "fossil carbon" range includes at its upper end methane hydrates from the ocean floor. The "oxygen limit" is the amount of fossil carbon that would use up all oxygen available in air for its combustion. Carbon consumption for the 21st century ranges from 600 Gt (current consumption held constant) to 2400 Gt. "Ocean acidic" and "ocean neutral" are the ocean's uptake capacities for carbonic acid and neutralized carbonic acid, respectively. The upper limits of capacity or lifetime for underground injection and mineral carbonates are not well constrained. EOR stands for enhanced oil recovery.

Lackner, K. S. 2003. A Guide to CO_2 Sequestration. Science 300:1677-1678.